4.3 Adsorbate induced surface core level shifts of metals

REINHARD DENECKE, NILS MÅRTENSSON

4.3.1 Introduction

Core level photoelectron spectroscopy is an element specific, surface sensitive and quantitative probe, which can be used to identify the elemental composition of surfaces. The primary information acquired is the electron binding energy. This binding energy depends strongly on the coordination of the respective atom and/or its neigboring atoms. These reflect the chemistry (alloys, oxides or adsorbates) around the atom from which the photoelectron is being emitted. Any differences in these parameters will lead to differences in the electron binding energy, and this change is called chemical shift.

The chemical shifts make it possible to distinguish between atoms of the same element in different chemical environments. Of particular interest for the investigation of surface systems is the surface core level shift (SCLS). When it became possible to measure core level photoelectron spectra with sufficiently high resolution and surface sensitivity it was realized that the different surroundings of the atoms at the surface and in the bulk of a sample lead to a chemical shift, the surface core level shift. The surface core level shifts may be further modified by the presence of adsorbed atoms and molecules. From these shifts most important information about the adsorbate-substrate bonding can be obtained. There exist some review articles dealing with parts of the material presented here [86Ege, 95Mar, 01And1, 03Bar2]. Nevertheless, they mainly cover only small fractions of the whole subject, either by concentrating on a specific substrate material, or by considering only data from a particular working group.

In the present contribution we review the existing measurements of adsorbate induced core level shifts. Surface core level shifts are present for all types of systems. However, we restrict ourselves to metallic substrates. We exclude semiconductor surfaces due to the fact that these often have very complex surface structures (reconstructions) and complex adsorbate arrangements. These situations would have to be described in much more detail than what is suited for this type of tabulation. For the same reason we exclude compound surfaces. We furthermore restrict ourselves to the adsorption of small (gas) molecules where each adsorbed atom or molecule bonds to a small and well-defined number of surface atoms. Large adsorbate molecules lead to a more distributed influence on the surface atoms and again each situation would have to be discussed in some detail. Furthermore, we only treat adsorbate overlayers. We do not cover for instance the growth of oxide films in general, but we will give some examples where we think it is appropriate. We also exclude metallic adsorbates except for alkali systems. The adsorption of metallic atoms often leads to complex situations, with a strong and often continuous dependence on coverage, and one would have to describe detailed phase diagrams for each system. The shifts for these situations are, however, well understood and for a discussion of these we refer to, e.g., [88Nil, 89Ste1, 89Ste2, 88Mar]. The case of alkali and earth-alkali metals is somehow special since in most cases they do not display typical metallic behavior. We have therefore included some examples.

In the tables of the data section we are exclusively dealing with experimental data. There are, however, a large number of theoretical studies on surface and adsorbate-induced core-level shifts as well. In the next section we will briefly outline some theoretical concepts and refer to some others. In the subsections of the data section we will give citations of the suitable theoretical articles and discuss them briefly, where appropriate. For more specific values the reader is also referred to cited publications in the respective experimental articles.

The surface core level shift

Chemical shifts for metallic systems are well understood theoretically. The final state system is identical to the initial state with the exception that one core electron is missing for one of the atoms in the system. This core-ionized atom is a different chemical species with different properties. Furthermore it has been shown that for metallic systems there is a complete screening of the core ionized state (e.g. [80Joh]). This implies that the valence electron distribution can be treated as fully adjusted to the new situation. When calculating core ionization energies one contribution corresponds to the energy of a (chemical) replacement reaction where the original atom is replaced by a core ionized one. In this section we derive an expression for the surface chemical shift, which can be used to make some general statements about the shifts. For a more detailed derivation we refer to, e.g., [80Joh, 83Joh, 88Nil, 95Mar].

The binding energy for a core level denoted c in a metal M is defined as the difference in total energy between the system with a core electron missing in shell c and the total energy of the initial state system

$$E_B(\mathrm{M, c}) = E_{Tot}(\mathrm{M, c}) - E_{Tot}(\mathrm{M}) \tag{1}$$

When discussing chemical shifts in metallic systems, one can make the following partitioning of the expression for the binding energy:

$$E_B(\mathrm{M, c}) = E_0(\mathrm{M, c}) + E_{Bond}(\mathrm{M}) - E_{Bond}(\mathrm{M_c, M}) \tag{2}$$

$E_{Bond}(\mathrm{M})$ is the energy by which an atom in the metal M bonds to the lattice. We use the sign convention that a stable metal corresponds to a positive value of $E_{Bond}(\mathrm{M})$. $E_{Bond}(\mathrm{M_c, M})$ is the corresponding energy for a core ionized atom $\mathrm{M_c}$ in the M metal host. $E_0(\mathrm{M, c})$ contains all other contributions to the core ionization energy. It can be shown that $E_0(\mathrm{M, c})$ is independent of the detailed coordination of the core ionized atom and that this quantity will cancel when chemical shifts are considered.

For the bulk and the surface of the metal M, Eq. (2) can be written as

$$E_B(\mathrm{M, c, bulk}) = E_0(\mathrm{M, c}) + E_{Bond,\ bulk}(\mathrm{M}) - E_{Bond,\ bulk}(\mathrm{M_c,M}) \tag{3}$$

$$E_B(\mathrm{M, c, surf}) = E_0(\mathrm{M, c}) + E_{Bond,\ surf}(\mathrm{M}) - E_{Bond,\ surf}(\mathrm{M_c, M}) \tag{4}$$

The surface core level shift is defined as

$$\Delta_s = E_B(\mathrm{M, c, surf}) - E_B(\mathrm{M, c, bulk}) \tag{5}$$

Before inserting (3) and (4) in (5) we make the following definitions

$$E_{Bond,\ surf}(\mathrm{M}) = \beta E_{Bond,\ bulk}(\mathrm{M}) \tag{6}$$

$$E_{Bond,\ surf}(\mathrm{M_c, M}) = \beta' E_{Bond,\ bulk}(\mathrm{M_c, M}) \tag{7}$$

β and β' are parameters that describe the effects of the reduced atomic coordination at the surface. Due to the reduced number of neighbors the bonding for a surface atom to the lattice will be smaller than for the bulk and hence β and β' are parameters with values <1. β and β' are of the order of 0.8 for a close-packed surface and smaller for more open surfaces. For the present qualitative discussion we assume that $\beta = \beta'$ and furthermore we rewrite this factor as $1 - \alpha$. Hence $\alpha \approx 0.2$. With these definitions and assumptions we arrive at the following expression for the surface core level shift

$$\Delta_s = \alpha (E_{Bond,\ bulk}(\mathrm{M_c, M}) - E_{Bond,\ bulk}(\mathrm{M})) \tag{8}$$

In order to evaluate this expression we first of all note that $E_{Bond,\ bulk}(M)$ is normally identical to the cohesive energy of the metal M. There are some exceptions where there are significant configuration changes between the free atom and the metal [80Joh]. This is for instance the case for several lanthanides. For the term $E_{Bond,\ bulk}(M_c, M)$ it has been shown that a first and fairly accurate approximation is obtained by considering the corresponding energy in a lattice where all M atoms are replaced by core ionized atoms, i.e. $E_{Bond}(M_c)$. Furthermore, a good estimate of this energy is obtained by noticing that the chemical properties of a core ionized atom are very similar to those of the next element in the Periodic Table. This is due to the fact that the valence electron distribution reacts in very much the same way upon the removal of a core electron as for the addition of a unit charge to the nucleus of the atom. $E_{Bond,\ bulk}(M_c, M)$ can thus be approximated by the cohesive energy of the next element in the Periodic Table [80Joh].

Surface core level shifts are typically of the order of a few tenths of an eV up to about one eV. In some systems the surface components shift to lower binding energies and in some systems they shift to higher binding energies. This can be understood from Eq. (8). For an early transition metal (to the left in the Periodic Table) the fully screened final state atom bonds stronger to the lattice than the initial state atom ($E_{coh}(M_{Z+1}) > E_{coh}(M_Z)$). This is due to the fact that one more valence electron is occupying a bonding orbital. This yields a positive surface core level shift (towards higher binding energies). For a late transition metal (to the right in the Periodic Table) the bonding of the final state atom is instead reduced due to an additional occupation of an unoccupied orbital. This leads to a negative shift. In order to illustrate this trend we show in Fig. 1 a compilation of measured and calculated SCLS for various 5d transition metals [89Mar]. Only values for close-packed surfaces are included. For a refined analysis of the surface core-level shifts one has to consider further details, such as the surface structure, and more specific details of the electronic structure [80Joh, 80Ros, 83Cit, 83Joh, 88Nil, 94Ald, 95Mar].

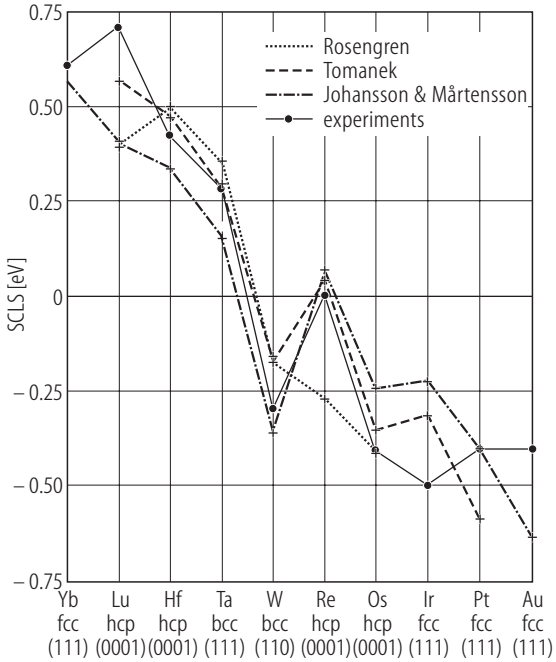

Fig. 1. Comparison of experimentally and theoretically determined SCLS's of the 5d transition metals. Only close-packed surfaces are included. Reproduced from [89Mar].

In this section we have presented an approximate evaluation of the shifts in order to give a qualitative account of trends in the surface core level shifts. However, the expressions in Eqs. (3) and (4) are exact and they serve as a powerful basis for detailed *ab initio* shift calculations using DFT (Density Functional Theory). In these calculations factors like the detailed surface structures can be included. Examples of this approach can be found in [93Bag, 94And2, 96Ham, 98Bih, 99Bag, 01Cho, 01Gan, 01Liz, 03Bir] and further references cited therein.

An important aspect of the chemical shifts in metallic systems is the fact that they are usually dominated by short-range effects. In most cases the main influence on the chemical shifts comes from the nearest neighbors. This makes the shifts very useful for many purposes, such as for obtaining information on the structural arrangements of the adsorbates. From the treatment above it is also clear how the influence of an adsorbate could be included in the shift calculations. In the presence of an adsorbate the terms $E_{Bond,\ surf}(M)$ and $E_{Bond,\ surf}(M_c, M)$ in Eq. (4) will contain contributions corresponding to the bonding of the adsorbate to a surface atom before and after the ionization, respectively. In this way we obtain the following modified expression for the core ionization energy for the adsorbate covered surface:

$$E_B(M, c, surf, ads) = E_B(M, c, surf) + E_{ads}(M) - E_{ads}(M_c, M) \quad (9)$$

We use the sign convention that E_{ads} is positive for a stable adsorbate. In this case it is not always straightforward to make simple quantitative statements about the shifts. $E_{ads}(M)$ is normally known. In the final state one of the M metal atoms has changed to an M_c atom and independent information about this situation is usually not available. In the case of on-top adsorption where the adsorbate bonds only to one substrate atom and assuming only nearest neighbor interaction, the last term can be written as $E_{ads}(M_c)$. If the atom or molecule bonds at this site also for the Z+1 metal independent information can be obtained also for this term. However, in the general case total energy calculations are required in order to calculate the shifts.

Based on the theoretical understanding of the core level shifts it has also been realized that the shifts are directly related to other most relevant properties of the systems. The surface core level shift has thus direct links to surface segregation energies [80Joh, 83Ege]. This implies that there is a similar connection between adsorbate induced surface core level shifts and adsorbate effects on the surface segregation energies [88Mar].

Binding energy scales

For the utilization of chemical shifts it is very important to define what reference energy is used for the shift scale. In this work we give all shifts relative to the bulk binding energies. The shift between the surface and the bulk components is usually seen directly in the spectrum. This way of using relative binding energies from the same measurement avoids all problems related to properly calibrating absolute energy scales. For each surface we present in the tables also the determined surface core level shift for the clean surfaces. In this way one can in each case derive by how much the surface components are shifted due to the presence of the adsorbates.

The utilization of the bulk component as the energy zero for the shift scale usually gives well-defined shift values. This choice is based on the assumption that the bulk binding energy can be accurately determined. This is usually a relevant assumption. In some cases there may be significant shifts also of one or more layers below the first surface layer. These are often unresolved and lead to a broadening of the bulk peak. If the measurements are performed under similar conditions in different investigations this way of establishing the reference energy does not introduce any additional errors since the same ratio of peaks from the different layers will be determined. However, if the measurements are different in terms of, e.g., surface sensitivity, the measurements will locate the bulk component at slightly different energies. Whenever a second layer shift has been identified also this value is included in the tables. Beryllium provides a striking example of the existence of shifts also for deeper layers. For the Be(0001) surface distinct and well resolved core level shifts are observed for the four outermost surface layers [01And2]. A spectrum with the deconvoluted components (“B” for the bulk and “S1”, “S2”, “S3”, “S4” for the outermost surface layers, counted from the surface) is shown in Fig. 2. This is, however, a rather unique case due to the semimetallic character of Be. Be is not included in the present review since no adsorbate measurements have been performed.

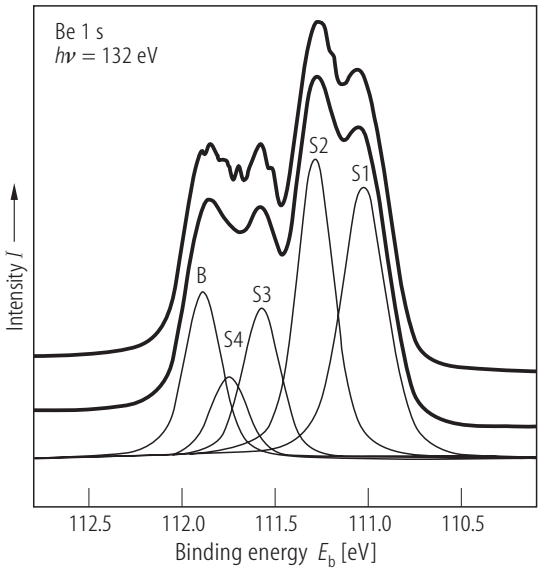

Fig. 2. Be 1s core level recorded at a photon energy of 132 eV measured with a resolution of 20 meV (upper curve) and 70 meV (lower curve). Included are the results of a deconvolution into the bulk component "B" and four outermost surface layers "S1", "S2", "S3", and "S4". The fine structure in the upper curve is due to vibrational excitation. Reproduced from [01And2].

Determination of surface core level shifts

One of the important issues is that of correctly determining the core-level line positions from the measured spectra. There are many contributions to the line profiles and furthermore these are not completely known. The shifts are also usually rather small compared to the line widths leading to overlapping spectral features. Basically one needs to fit a model line profile to each core electron line in the system. If all contributions are well described by these model line profiles the determined core level positions are also well defined. Since there is no strictly unique way to determine core level binding energies, it is important that one reports how the binding energies have been determined. When determining surface core level shifts many line-shape contributions are similar for the different core level peaks. Several of the broadening contributions are similar for a surface, with or without an adsorbate, and for the bulk of the metal. This makes the shift determinations less model dependent than the determination of the absolute binding energies. This also implies that the shifts are transferable from one investigation to another. What is furthermore improving the situation very much is, that one is considering shifts between atoms in very similar environments.

The core electron line profiles can be described as a convolution of a number of broadening functions. Several of these are due to effects which are intrinsic to the core ionization process. First of all a core excitation has a finite lifetime. This usually leads to a Lorentzian contribution to the line profile. This is the case for all core levels that are used for detailed determinations of chemical shifts. The Lorentzian broadening is totally symmetric. Usually the Lorentzian broadening can be considered to be identical for a core level independent of the chemical environment. The Lorentzian function can be described as follows:

$$L(E, E_0, \lambda) \propto 2\lambda/[\lambda^2-(E-E_0)^2] \tag{10}$$

E_0 denotes the peak position, 2λ is the full width at half maximum (FWHM).

The creation of a core-hole at the surface or in the bulk of a metal leads to a disturbance of the lattice. This will generate replicas of the core electron line, shifted by the energy required to excite one or more phonons in the system. Usually this leads to unresolved spectral features and the net result is a broadening of the core electron lines. In the case of Be, however, distinct phonon side bands have been resolved (see Fig. 2). In most cases many phonons are excited and the net broadening is to a good approximation a symmetric Gaussian:

$$G(E, E_0, \sigma) \propto 1/[\sqrt{(2\pi)}\sigma] \exp[-(E-E_0)^2/(2\sigma^2)] \quad (11)$$

Here, 2σ is the FWHM, E_0 is again the peak position.

The core ionization process also leads to the excitation of valence electrons. These processes are denoted shake-up and shake-off. For a metallic system there is a continuum of excitation energies all the way down to zero. This leads to asymmetric line-shapes with tails towards the high binding energy side of the core level spectra. The resulting line-shapes depend on the details of the electronic structure of the system. However, usually the line profiles can be well described by model line profiles with one or possibly two parameters. One such description was introduced by Doniach and Šunjić [70Don] (D-S):

$$DS(E, \gamma, \alpha) \propto \Gamma(1-\alpha)\cos[\pi\alpha/2+(1-\alpha)\arctan(E/\gamma)]/[(E^2+\gamma^2)^{(1-\alpha)/2}] \quad (12)$$

with 2γ being the Lorentzian FWHM, and α describing the asymmetry parameter. This time, $E_0 = 0$ is assumed.

There is also a contribution in the spectra due to photoelectrons which have undergone inelastic scattering processes after the core ionization. Also this contribution leads to an asymmetric broadening towards the low kinetic energy or high binding energy side. These two contributions usually cannot be separated in a straightforward manner.

In some cases there may also be discrete shake-up states in the vicinity of the main lines. There may also be other intrinsic line-shape contributions. In some systems there are effects due to the coupling between the open core shell created by the removal of a core electron and open valence shells. This may lead to complex final state spectra. The problem of unresolved shifts for different atomic layers was also discussed above.

A most important contribution is that caused by the finite resolution of the experimental setup. This is due to the energy profile of the exciting photon spectrum as well as the finite resolution of the electron analyzer. This may lead to different types of line-shapes which also depend on the experimental setup. However, in most cases the instrumental broadening is reasonably well described by a Gaussian line profile (see Eq. 11). However, if shift measurements are performed at very different energy resolution any inaccuracies in the used model line profiles will lead to differences in the determined shifts.

For the final fitting procedure convolutions of the various broadening effects have to be calculated. For a symmetric line this results in the Voigt profile which is a convolution between a Gaussian and a Lorentzian line profile, whereas for asymmetric line shapes a D-S function is convoluted with a Gaussian function.

As a word of caution we want to emphasize again that fitting procedures not necessarily produce unique results. In fact, changing the number of components or changing some constraints (like going from variable peak positions to fixed ones) can easily change binding energy values by significant amounts. Therefore, the values quoted in the tables below should be used with this in mind. For further specific fitting procedures the reader is referred to the original articles. We have chosen not to describe, discuss and evaluate these in connection with the tabulations.

Systematics of surface core level shifts

For the tabulation of adsorbate-induced surface core level shifts it is important to describe the adsorbate structures correctly. We refer in each case to the original reference for details of the structures. Whereas for the adsorbate itself a classification according to the binding site seems to be the most relevant one, this does usually not provide sufficient information to describe the situation for the substrate atoms involved.

When comparing different adsorbate-induced surface core-level shifts and identifying trends in these it may be helpful to describe and quantify the surface atom coordination to the adsorbed atoms or molecules. We have included this type of analysis in those cases where it is published. As a parameter we have used the coordination number n_{ads} of the metal surface atoms to the adsorbates. It is based on the assumption that an adsorbate of a particular kind and for a particular type of surface has a well-defined total influence on the substrate atoms. This influence, in turn, is very much localized to the nearest-

neighbor atoms [88Nil, 91And, 00Sur, 01Gan]. An on-top adsorbate gives n_{ads} = 1 for the atom to which it is attached and n_{ads} = 0 for all other atoms. For a bridge bonded species the influence is shared between the two substrate atoms and both of these get a contribution of n_{ads} = 1/2. Furthermore, the influence is considered to be additive. This implies, for instance, that a surface atom that has two bridge bonded adsorbates attached to it gets n_{ads} = 1.

There is no strict physical support for this model. In fact, it does sometimes not even work for very similar systems. However, there are several systems for which it provides a fairly reasonable way of systemizing and rationalizing the observed shifts. In brief, one could state that it seems to be applicable for atomic oxygen and CO adsorption. In the case of oxygen adsorption on Rh(111) a combined experimental and theoretical investigation using this concept has been performed [01Gan]. Oxygen adsorbs in threefold hollow sites on this surface. The different adsorbate phases correspond to situations with Rh surface atoms bonding to one, two or three oxygen atoms. These Rh sites correspond to n_{ads} = 1/3, n_{ads} = 2/3 and n_{ads} = 1, respectively. The p(2×2)-O phase has an adsorbate coverage of 0.25 ML and consists of 25 % surface atoms with n_{ads} = 0 and 75 % of atoms with n_{ads} = 1/3. In the p(2×1)-O phase (0.5 ML) there are 50 % surface atoms with n_{ads} = 1/3 and 50 % with n_{ads} = 2/3. It was found that the peaks in the spectra can be identified according to the parameter n_{ads}. The fact that surface atoms in different situations but with the same n_{ads} undergo approximately the same shift gives strong evidence that the shifts are dominated by nearest neighbor interaction. Furthermore, it was found that each bond to oxygen shifts the Rh 3d core level of a substrate atom by about 0.3 eV. A theoretical analysis of this correlation was also made [01Gan].

In an analysis of CO on Pd(111) a similar simple relationship was found [00Sur]. Typical spectra are shown in Fig. 3. In this case the core level data could be used to distinguish between different proposed models for the adsorbate structures. In this system different adsorption sites are populated. In the (√3×√3)R30° phase (0.33 ML adsorbate coverage) each surface atom is ideally attached to one CO bonded in a threefold hollow site ("H1"), yielding n_{ads} = 1/3. Also for the c(4×2)-2CO phase (0.5 ML) there are only hollow site adsorbates. There are 50 % Pd surface atoms with n_{ads} = 1/3 ("H1") and 50 % with n_{ads} = 2/3 ("H2"). In the (2×2)-3CO phase (0.75 ML) there is instead a mixture of hollow and on-top sites ("T"). In this case 75 % of the Pd surface atoms bond to two hollow site CO molecules corresponding to n_{ads} = 2/3. The remaining 25 % of the surface atoms bond to one on-top adsorbate giving n_{ads} = 1. For intermediate coverages CO is also found on bridge sites ("Br"), as seen in the top panel of Fig. 3; here, n_{ads} = 1/2. Also in this case the shifts correlate fairly well with n_{ads}. This is the case in spite of the fact that different adsorption sites are involved [00Sur]. However, the clean surface with n_{ads} = 0 does not fit to the proposed linear dependence between core-level shift and n_{ads}, in contrast to the case of O/Rh(111) (see discussion above).

Experimental requirements

In order to observe the adsorbate-induced surface core-level shifts of interest here, the experimental conditions have to be such, that the photoemission signal is tuned to be quite surface sensitive. Since the critical parameter is the kinetic energy of the released photoelectron [79Sea], this sensitivity varies with the binding energy of the core level under study and with the excitation energy used. Thus, for a special choice of levels laboratory photon sources with fixed energy sometimes yield very good results [86Duc]. In most cases, however, synchrotron radiation is the photon source of choice for these high-resolution experiments. Synchrotron radiation is tunable in energy and with state-of-the-art monochromators high energy resolution (up to $E/\Delta E$=10000) can be achieved (see for example [99Den]).

Another limiting factor is the width of the core-level lines. Depending on the natural lifetime and its related peak width it may be difficult to resolve surface related contributions, even with high resolution of the exciting radiation. Typical examples of these inherently wide lines are p levels, as e.g., encountered in Ni or Cu. This is reflected in the lack of experimental data for these systems. In contrary, the d and especially the f levels are quite narrow and thus yield well separated core-level components.

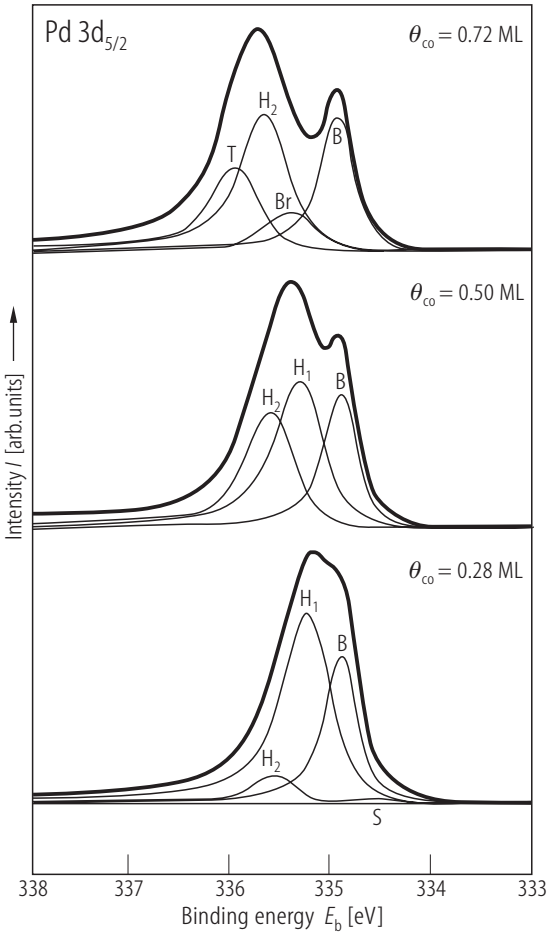

Fig. 3. Pd $3d_{5/2}$ core level spectra recorded with a photon energy of 400 eV for varying CO coverages at a sample temperature of 120 K. Components described in the text are also inlcuded. "B" marks the bulk emission, "S" the clean surface component. Peaks "H1" and "H2" are related to Pd atoms bonded to one or two CO molecules in threefold hollow sites, component "Br" is due to Pd atoms in contact with CO in a bridging position, and peak "T" represents Pd atoms with CO in on-top position. Reproduced from [00Sur].

The apparent intensity of the different contributions can also influence the possibility to clearly identify adsorbate-induced features. In this respect, energy-dependent photoelectron diffraction plays an important role (see, e.g., [02Woo] and references therein). Again, the tunability of the photon energy allows to use kinetic energies which emphasize the contributions of interest. The detection angle of the photoelectrons (usually measured relative to the surface normal) also has a drastic effect on the surface sensitivity. The more grazing the escape angle, the more surface sentitivity is obtained. Additionally, again photoelectron diffraction effects, but now in the angular distribution, can further change relative intensities of different contributions [97Fad]. Being able to change this detection angle is an elegant way to identify surface related features, as is done in most of the studies using laboratory sources.

Another important aspect in the studies summarized in this contribution is the cleanliness of the sample. Possible undetected surface contaminations not only strongly suppress the surface component, but can also lead to new features which are mistakenly interpreted as clean surface components. On the other hand, unwanted coadsorbates could also alter the binding energy of a certain adsorbate under study, thus leading to wrong values. These difficulties are usually more pronounced on more reactive metals, such as Aluminum. Therefore, discrepancies in the published data can also be caused by varying contamination levels.

4.3.2 Data section

In this chapter we present an overview of the reported values for adsorbate-induced surface core-level shifts. As mentioned in the introduction, we are giving the shifts relative to the bulk peak, which is the natural reference level. Since the shifts are closely related to the clean surface core-level shifts, we are including values for this as well. However, since measuring absolute binding energies in a reliable and comparable way is rather difficult, we will only quote difference values with respect to the individually reported bulk binding energies. If, for orientation only, absolute binding energy values of the bulk components are included, they are referenced to the Fermi energy. We use the convention that increasing binding energies ("stronger binding") are denoted by larger positive numbers. Please note that some authors are using a scale going to more negative values. If that is the case we have "converted" the values accordingly. We will only quote numerical values given in the publications, and have not derived values from figures. Accuracies (quoted number of digits) are taken from the literature, but no error margins are given in our tables.

As will be noticed, there are remarkable differences in some reported values. Sometimes they are due to improved experimental resolution with easier identification of components in the line shapes. Sometimes the origin of these differences is not clear. While some publications try to explain these disagreements with varying sample cleanliness or different sample preparation procedures, we are not commenting on differing results. Interested readers are referred to the original articles. As suggested guideline, more recent publications are more likely to quote more reliable numbers, but not necessarily.

For each surface plane we will summarize the binding energy shifts in a separate table, ordered by adsorbate. For each adsorbate we will use the reported adsorbate binding configurations, if possible. In order to improve the readability we use the following abbreviations: H for hollow sites, T for on-top sites, B for bridge sites. This assignment of the adsorption site is rather difficult since we are dealing with the substrate atoms just influenced by the adsorbates. In some cases we will see that a correlation to adsorbate binding site is not possible. In those cases we give the different substrate atom types as quoted by the respective reference. For more general remarks, see the Introduction. We will discuss further details in the respective subsections.

Data for the 3d transition metals are rather scarce. The 3d metals are more difficult to measure at high resolution than the narrowest levels for the 4d and 5d metals. This is due to the fact that the narrowest core-electron lines, the 2p lines, have rather high binding energies. This implies that higher photon energies are needed which limits the resolution. The 2p electron lines for the 3d transition metals are also intrinsically broader than the narrowest lines for the 4d and 5d transition metals as well as for the narrowest lines of all simple metals [81Nyh]. The intrinsic lifetime broadening is slightly larger. However, the additional broadening has mainly other reasons. One reason is the narrow band character of the 3d band. The 2p-3d coupling in the spectroscopic final states leads to a more complex line shape of the core-levels in the 3d metals. These effects do not lead to resolved effects in the spectra but are only seen as additional broadenings of the core electron lines. These make any surface core level shift harder to resolve.

Below we show an example of a table given for the various substrates. In the beginning we display the quoted binding energies of the respective substrate bulk core level, with respect to the Fermi level. If there are different published values, we will give all of them. In the next row the clean surface core-level shift is given. As mentioned in the introduction, the shifts are all given relative to the respective bulk binding energies. Here, the 1st column gives details about the position of the substrate atoms considered. "1st layer" denotes the obvious surface layer, while "2nd layer" refers to the first underlayer, if it is distinguishable from the bulk value.

Values for different adsorbates are given in the following rows, grouped in sections. The columns are organized as follows. The first column gives a short description of the adsorbate layer structure and the adsorption site or bonding configuration considered. We reproduce the classification used in the cited publication, even if it has been proposed to be wrong by more recent publications. If applicable, the next column gives the (fractional) coordination number of the substrate surface atom considered. The 3rd column gives the coverage for the adsorbate structure under consideration. This is usually the ideal (nominal) value, not the value obtained in the actual experiment. Here, 1 ML is defined as one adsorbate

molecule/atom per substrate surface atom. The 4th column displays the values of the core-level shifts in units of eV. If different values exist in the literature, we give all of them without commenting on possible reasons for the discrepancies. The number of digits quoted is from the original reference, but no error bar values are reported. The last column gives the cited references and the line shapes used in the data analysis; if no fitting procedure has been used, we will also notice. The used abbreviations are as follows: "D-S": Doniach-Sunjic line shape; "+G": additional Gaussian function; "V": Voigt profile; "Sci": fitting routine supplied by Scienta, using an asymmetric line profile with a combined FWHM and a ratio of Lorentzian and Gaussian contributions; "no fit": no fitting routine has been used by the authors. "special" denotes line shapes used by only one working group; for details see the original paper. If the line shape is not specified in the original paper ("n.s."), the data are deconvoluted, but but no details are given.

Example:

Ta $4f_{7/2}$ level, E_b(bulk)			21.65 eV	Ref. 1, 2 (D-S+G)
Clean surface				
1st layer 2nd layer			+0.74 eV +0.14 eV	Ref. 1, 2 (D-S+G)
atomic O adsorption				
O chemisorbed		low coverage	+0.99 eV	Ref. 1 (D-S+G)
O oxide-like		higher coverage	+1.29 eV	Ref. 1 (D-S+G)
H adsorption				
H		low coverage	+0.93 eV	Ref. 1 (D-S+G)

The different substrates are listed in the following sections in the order of their appearance in the Periodic Table. Within each substrate system, (100), (110) and (111) surface orientations are shown in this order. If values for stepped surfaces exist, they are displayed next. The different adsorbates considered for the various substrates are not given in a special order. Usually the adsorbed species is given, not the gas phase molecule used in the experiment. With a few exceptions, only substrates are included for which adsorbate data have been published. There are some additional substrate surfaces, for which either only clean surface measurements or only theoretical investigations exist; they are not listed here.

4.3.2.1 Al(001)

In a theoretical study using the linearized augmented-plane-wave (LAPW) method a negligible clean surface core-level shift was found, whereas for a p(1×1)-O layer a shift of −1.5 eV was predicted [81Kra]. From a slightly more sophisticated full-potential self-consistent LAPW (FLAPW) calculation including crystal field splitting effects, a continuous shift for the first four surface layers was predicted, with a value of −0.12 eV for the surface layer [81Wim].

Al $2p_{3/2}$ level, E_b(bulk)			73 eV 72.26 eV	78Bac (no fit) 91Bag (n.s.)
Clean surface				
			+0.22 eV	91Bag (n.s.)
			–0.096 eV	91Nyh (D-S+G)
O adsorption				
O chemisorbed			not seen	78Bac (no fit)
subsurface oxygen			+1.4 eV	78Ebe (no fit)
Al_2O_3			+2.6 eV	78Bac (no fit)
Al_2O_3			+2.7 eV	78Ebe (no fit)

Alkali adsorption				
Na c(2×2) 100K, 4-fold hollow		0.5 ML	–0.150 eV	92And (no fit)
Na c(2×2) RT - highly coord.			–0.500 eV	92And (no fit)
Na c(2×2) RT - less coord.			–0.115 eV	92And (no fit)

4.3.2.2 Al(111)

Aluminum as a very reactive metal has caused some attraction in the context of the oxide formation. Although we do not generally deal with oxides in this contribution, we have included the bulk oxide values for comparison here. The species denoted "subsurface oxygen" is most likely identical to a surface oxide.

The preparation in [93Ber] was basically a room temperature oxidation process. The various peaks could be assigned to some chemisorbed species and some "bulk oxide", which in fact seems to be a surface oxide. The peak with a shift of –0.14 eV was proposed to be due to Al atoms at the interface between the Al crystal and the surface oxide network. It is not bonded to any oxygen [93Ber].

Al $2p_{3/2}$ level, E_b(bulk)			73 eV	78Flo, 78Bac (no fit)
Clean surface				
			< 0.015 eV	91Nyh (D-S+G)
O adsorption				
Al at interface, no O bond			–0.14 eV	93Ber (D-S+G)
O chemisorbed, Al-1O			+0.37 eV	93Ber (D-S+G)
O chemisorbed, Al-2O			+0.84 eV	93Ber (D-S+G)
O chemisorbed, Al-3O			+1.37 eV	93Ber (D-S+G)
O chemisorbed (3-fold hollow)		1 ML	+1.3 eV	95Ruc (no fit)
(1 × 1) overlayer [79Ebe]			+1.4 eV	78Flo, 78Bac, 79Bia, 79Ebe (no fit)
subsurface oxygen			+2.7 eV	95Ruc (no fit)
surface oxide			+2.7 eV	78Flo, 78Bac, 79Bia, 79Ebe (no fit)
"bulk oxide"			+2.63 eV	93Ber (D-S+G)
Al_2O_3			+3.5 eV	95Ruc (no fit)
Al_2O_3			+3.3 eV	79Bia (no fit)
Alkali adsorption				
Cs (2×2)			–0.130 eV	93And (no fit)
Cs (√3×√3)			–0.145 eV	93And (no fit)
Rb (2×2)			–0.130 eV	93And (no fit)
Rb (√3×√3)			–0.140 eV	93And (no fit)
K (√3×√3)		0.33 ML	–0.130 eV	93And (no fit)
Na (3×3)			–0.070 eV	93And (no fit)
Na (4×4)			–0.080 eV	93And (no fit)
Na (√3×√3)			–0.130 eV	93And (no fit)

4.3.2.3 Ni(100)

The problem of accurately resolved surface core level shifts for the 3d transition metals was discussed in the introduction to this section. The measurements in [93Nil] give shifts for the main line as well as for the so-called "6 eV satellite". These represent differently screened final states.

Ni $2p_{3/2}$ level, E_b(bulk)			852.60 eV 852.77 eV	93Nil (no fit) 84Ege (no fit)
Clean surface				
main line			–0.3 eV	93Nil (no fit)
satellite			–0.7 eV	93Nil (no fit)
not specified			–0.43 eV	84Ege (no fit)
CO adsorption				
c(2×2) on-top - main line		0.5 ML	+0.7 eV	93Nil (no fit)
satellite			+1.5 eV	93Nil (no fit)
c(2×2) - not specified		0.5 ML	+0.24 eV	84Ege, 85Ege (no fit)
H adsorption				
c(2×2)			–0.36 eV	85Ege (no fit)
O adsorption				
c(2×2)		0.5 ML	–0.18 eV	84Ege, 85Ege (no fit)

4.3.2.4 Mo(110)

Mo $3d_{5/2}$ level, E_b(bulk)			227.9 eV	95And (n.s.)
Clean surface				
			–0.33 eV	95And (n.s.)
			–0.333 eV	93Lun (D-S+G)
Na adsorption				
		saturated ML	–0.33 eV	95And (n.s.)

4.3.2.5 Ru(0001)

Oxygen on Ru(0001) is a prototype system. Oxygen atoms occupy hcp hollow sites only, thus making it necessary to think about the correlation of peak components and bonding situations. This has been done in terms of coordination number, as has been discussed in Sect. 4.3.1 already. “1O”, “2O”, and “3O” denote Ru atoms coordinated to one, two, and three oxygen atoms, respectively. In [01Liz] the spectra for all coverages are fitted including the 1st and 2nd layer clean surface peaks. The binding energy values for these peaks change slightly as well with changing oxygen coverage. However, for clarity we do not include these values here. Just briefly, the 1st layer clean surface component vanishes for coverages higher than 0.25 ML, while the 2nd layer component is still close to its clean surface value up to coverages of 0.75 ML. For the (1×1)-O structure the 2nd layer Ru atoms get coordinated to one oxygen as well, thus shifting to a position identical to the bulk Ru position. The behavior observed experimentally is also described theoretically by DFT calculations, yielding very similar values for the core-level shifts [01Liz].

The case of RuO_2 (110) has been included, since it is discussed in close relationship with the oxygen adsorption [01Ove]. In addition, the so-called coordinationally unsaturated (cus) Ru atoms on the surface of this oxide are rather much involved in the oxide formation, as judged by their large binding energy difference with respect to the surface Ru atoms of the clean surface (see table below). Within this study, the adsorbate-induced core-level shifts have also been calculated, taking both initial state and final state contributions into account. Qualitatively the results follow the trend in the experimental values, slightly overestimating the shift [01Ove].

Ru $3d_{5/2}$ level, E_b(bulk)			280.1 eV	01Liz, 01Ove (D-S+G)
Clean surface				
1st layer 2nd layer			–0.366 eV +0.125 eV	01Liz (D-S+G)
1st layer 2nd layer			–0.363 eV +0.135 eV	97Sti (Sci)
O adsorption				
p(2×2) 1O	1/3	0.25 ML	+0.020 eV	01Liz (D-S+G)
p(2×1) 1O	1/3	0.50 ML	–0.050 eV	01Liz (D-S+G)
p(2×1) 2O	2/3	0.50 ML	+0.390 eV	01Liz (D-S+G)
		0.5 ML	+0.40 eV	01Ove (D-S+G)
(2×2)-3O 2O	2/3	0.75 ML	+0.387 eV	01Liz (D-S+G)
(2×2)-3O 3O	3/3	0.75 ML	+0.980 eV	01Liz (D-S+G)
(1×1)-O 3O 1st layer	3/3	1 ML	+0.960 eV	01Liz (D-S+G)
		1 ML	+0.93 eV	01Ove (D-S+G)
(1×1)-O 1O 2nd layer		1 ML	0	01Liz (D-S+G)
(2×1) (not res.)			+0.371 eV	97Sti (Sci)
RuO_2 (110) - oxide RuO_2 (110) - cus			+0.63 eV +0.35 eV	01Ove (D-S+G)
CO adsorption				
not specified			–0.353 eV	97Sti (Sci)
H adsorption				
(1×1)			–0.254 eV	97Sti (Sci)
(2×1) - 1st layer 2nd layer			–0.304 eV +0.113 eV	97Sti (Sci)
NO+O coadsorption				
NO+2 O			+0.341 eV	97Sti (Sci)
NO+O - "1st layer" "2nd layer"			+0.530 eV +0.756 eV	97Sti (Sci)

4.3.2.6 Ru $(10\bar{1}0)$

In contrast to the papers about Ru(0001), where the binding energy of the bulk component of the Ru $3d_{5/2}$ level was given explicitly, the references on Ru $(10\bar{1}0)$ give no absolute binding energy values. From [00Bar2] we have taken from the figure the value of 280.1 eV, which also corresponds to the value reported for the Ru(0001) surface. Oxygen is again adsorbed in hcp hollow sites. "1O" and "2O" denote Ru atoms bonded to one or two O atoms.

Ru $3d_{5/2}$ level, E_b(bulk)			280.1 eV	00Bar2 (D-S+G)
Clean surface				
1st layer 2nd layer			–0.480 eV –0.240 eV	00Bar1, 00Bar2, 01Bar (D-S+G)
O adsorption				
c(4×2) 1O (2nd layer) (2×1)p2mg 1O (2nd layer)		all coverages	+0.465 eV	00Bar2, 01Bar (D-S+G)
c(4×2) 1O (1st layer)		<0.5 ML	–0.085 eV	00Bar2, 01Bar (D-S+G)
(2×1)p2mg 2O (1st layer)		>0.5 ML	+0.215 eV	00Bar2, 01Bar (D-S+G)

4.3.2.7 Rh(100)

CO adsorption gives rise to two clearly resolved states in C 1s core-level emission. However, in the Rh $3d_{5/2}$ level only three components due to bulk, clean surface and adsorbate covered Rh atoms are observed [98Str]. From a comparison between Rh $3d_{5/2}$ and C 1s spectra the on-top contribution is proposed to overlap with the bulk component.

Rh $3d_{5/2}$ level, E_b(bulk)			307.3 eV 307.6 eV	98Str (D-S+G) 94Bor (D-S+G)
Clean surface				
			–0.65 eV	98Str (D-S+G)
			–0.62 eV	94Bor (D-S+G)
			–0.64 eV	97Pri (D-S+G)
			–0.655 eV	96Zac (D-S+G)
CO adsorption				
on-top c(2×2)		0.5 ML	< ±0.05 eV	98Str (D-S+G)
"split (2×1)"		saturation	0	96Zac (D-S+G)
bridge		> 0.5 ML	–0.300 eV	98Str (D-S+G)
O adsorption				
O hollow (2×2)p4g		0.5 ML	–0.25 eV	96Zac (D-S+G)
NO adsorption				
NO			+0.385 eV	96Zac (D-S+G)
H adsorption				
H			–0.47 eV	96Zac (D-S+G)

4.3.2.8 Rh(110)

Rh $3d_{5/2}$ level, E_b(bulk)				
Clean surface				
			–0.65 eV	94Pri (D-S+G)
CO adsorption				
(2×1)p2mg			–0.08 eV	94Pri (D-S+G)
H adsorption				
20 L			–0.35 eV	94Pri (D-S+G)

4.3.2.9 Rh(111)

For oxygen adsorption, three types of Rh surface atoms are considered (see Fig. 4): type "A" for clean Rh, type "B" for Rh coordinated to one O adatom, type "C" for Rh coordinated to two O adatoms [01Gan]. A linear relationship between the core-level shift and the number of O neighbors can be observed; approximately one finds 0.3 eV per bond. This is very well reproduced by the calculations. The theoretical prediction for Rh coordinated to three O adatoms (type "D") in a (1×1) layer with 1 ML coverage is +0.94 eV.

In the case of CO adsorption, [98Beu] does not give coordination numbers. If we calculate these, we get 1 for on-top and 2/3 for the hollows in the (2×2) structure. That does not give a linear relationship, not even with respect to the clean surface component.

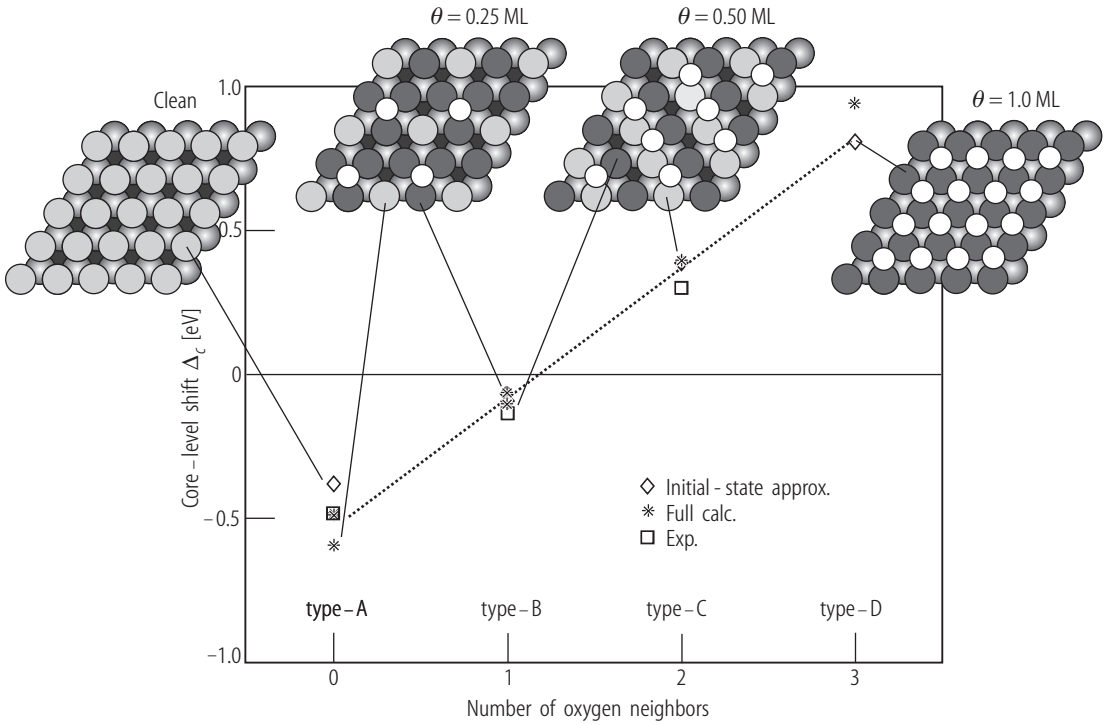

Fig. 4. Core-level shift relative to bulk signal for O adsorption on Rh(111). Comparison between experiment and theory is shown; reproduced from [01Gan].

For Rh(111) a number of theoretical studies exist as well. While some concentrate on the clean surface core-level shift [82Fei, 94And2], obtaining values close to the experimentally observed –0.5 eV, others also calculate adsorbate induced shifts [03Bir]. For CO/Rh(111), results of 0.24 eV for the on-top species in a (√3×√3)R30° structure and –0.22 eV for threefold hollow sites in the high coverage (2×2)-3CO phase [03Bir] agree very well with experimental values listed below. As shown above, also for O adsorption the theoretical description seems to work well [01Gan].

Rh $3d_{5/2}$ level, E_b(bulk)			307.18 eV	94And2, 98Beu (D-S+G)
Clean surface				
			–0.50 eV	94And2, 97Beu, 98Beu (D-S+G)
			–0.485 eV	01Gan (D-S+G)
1st layer 2nd layer			–0.46 eV +0.071 eV	03Bar (D-S+G)
CO adsorption				
(√3×√3)R30° on top		0.33 ML	+0.27 eV	97Beu, 98Beu (D-S+G)
(2×2)-3CO hollow		0.75 ML	–0.22 eV	98Beu (D-S+G)
O adsorption				
p(2×2) B hollow	1/3	0.25 ML	–0.140 eV	01Gan (D-S+G)
p(2×1) C hollow	2/3	0.5 ML	+0.295 eV	01Gan (D-S+G)
Alkali adsorption				
K, Rb, Cs			–0.50 eV	95And (n.s.)

4.3.2.10 Stepped Rh surfaces

The (111) terraces of the stepped surfaces exhibit a different SCLS as the Rh(111) surface, approaching the flat surface value with increasing terrace width. O adsorption on the steps gives rise to a binding energy shift of the step atoms only [03Gus].

Rh $3d_{5/2}$ level, E_b(bulk)			307.15 eV	03Gus (D-S+G)
Clean surface				
terrace (553)			–0.43 eV	03Gus (D-S+G)
terrace (151513)			–0.48 eV	03Gus (D-S+G)
step			–0.72 eV	03Gus (D-S+G)
underneath step			–0.14 eV	03Gus (D-S+G)
O adsorption				
step adsorption (553)		0.06 ML	–0.35 eV	03Gus (D-S+G)

4.3.2.11 Pd(100)

The case of CO on Pd(100) has been studied in some detail [91And]. There are two interesting aspects. First of all, there seems to be a linear relationship between the number of adsorbed CO molecules and the binding energy shift, increasing from 0.5 eV for one CO neighbor (called "bridge 1", coord. 1/2) to about 1.0 eV for two CO neighbors ("bridge 2", coord. 1). The other interesting aspect is that the binding energies of both Pd species change slightly with increasing coverage, i.e., with next nearest neighbors. A similar effect is also observed for other systems (e.g., CO on Pd(111)).

In [94Gur] no spectrum of the clean surface is shown. Therefore it is not possible to check the value given for the core-level shifts. However, we assume that the given SCLS is meant to be towards lower binding energies (–0.41 eV), despite the given value of +0.41 eV.

As stated by some of the authors [92Nyh, 94And2], the D-S line shape does not adequately describe the Pd 3d core level, due to the details of the density of states close to the Fermi level. Therefore, some groups use subtraction procedures which are labelled as "no fit". However, the same authors often use a D-S+G line shape for comparison as well. If discrepancies are small, we give only one value for the binding energy shift.

Pd $3d_{5/2}$ level, E_b(bulk)			334.95 eV 334.99 eV 334.96 eV	91And (D-S+G) 02Jaw2 (no fit) 94Gur (Sci) 96Par (no fit)
Clean surface				
			–0.43 eV	91And, 02Jaw2
			–0.44 eV	92Nyh (no fit)
			–0.41 eV	94Gur (Sci)
			–0.40 eV	02Jaw1 (no fit)
CO adsorption				
p(2√2×√2)R45° bridge 1	1/2	0.50 ML	+0.48 eV	91And (D-S+G)
p(3√2×√2)R45° bridge 1	1/2	0.67 ML	+0.56 eV	91And (D-S+G)
p(3√2×√2)R45° bridge 2	1	0.67 ML	+0.97 eV	91And (D-S+G)
p(4√2×√2)R45° bridge 1	1/2	0.75 ML	+0.60 eV	91And (D-S+G)
p(4√2×√2)R45° bridge 2	1	0.75 ML	+1.04 eV	91And (D-S+G)
unspecified CO			+0.47 eV	96Par (no fit)

O adsorption				
c(2×2) 4-fold hollow		0.5 ML	+0.55 eV +0.61 eV	96Par (no fit) 96Par (Sci)
c(2×2) 4-fold hollow		0.5 ML	+0.55 eV	94Gur (Sci)
NO adsorption				
p(4×2) 4-fold hollow		0.25 ML	+0.3 eV	02Jaw1 (no fit)
p(2√2×√2)R45° bridge		0.5 ML	+0.8 eV	02Jaw1 (no fit)
saturation		0.65 ML	+1.0 eV	02Jaw1, 02Jaw2 (no fit)
unspecified NO			+0.5 eV	96Par (no fit)
H adsorption				
c(2×2)		saturation	≈0 eV	92Nyh (no fit)
Alkali adsorption				
Na			+0.7 eV	95And (n.s.)

4.3.2.12 Pd(110)

CO on Pd(110) is a system that shows a reconstruction of the substrate for adsorption at room temperature. The Pd surface is still unreconstructed for CO coverages up to 0.3 ML. For CO coverages larger than 0.3 ML, a missing-row (1×2) reconstruction is found [97Ram], which coexists with the (1×1) structure up to coverages of 0.75 ML. For 0.75 ML (the saturation coverage at room temperature) the missing-row reconstruction of the substrate is complete. For higher coverages reachable at lower adsorption temperature or higher ambient pressures, the reconstruction is lifted again and CO forms the (2×1) p2mg structure [97Ram]. In [97Ram] only an averaged CO induced core-level position could be determined, leading to a continuous energy shift between 0.3 and 0.75 ML. The high coverage phase had to be prepared separately so that no information about the coverage range between 0.75 ML and 1 ML is given.

The authors of [96Bon] use exponentially-modified Gaussian line shapes for thr deconvolution of the different contributions.

Pd $3d_{5/2}$ level, E_b(bulk)			335.3 eV 335.2 eV	97Ram (Sci) 91Com (D-S+G) 96Bon (special)
Clean surface				
			–0.5 eV	97Ram (Sci)
			–0.24 eV	91Com (D-S+G)
			–0.55 eV	94And2 (no fit)
			–0.4 eV	96Bon (special)
CO adsorption				
randomly, unrec. substrate		<0.3 ML	+0.45 eV	97Ram (Sci)
(4×2)		0.75 ML	+0.63 eV	97Ram (Sci)
(2×1)p2mg bridge		1 ML	+0.94 eV	97Ram (Sci)
(2×1)p2mg bridge		1 ML	+0.93 eV	94Loc (D-S+G)
(2×1)p2mg bridge		1 ML	+0.98 eV	91Com (D-S+G)
(2×1)p2mg bridge		1 ML	+0.95 eV	96Loc (D-S+G)
O adsorption				
c(2×4) bridge		0.25 ML	+0.48 eV	91Com (D-S+G)
O_2 at 400 K (1×10^{-4} mbar)		22800 L	+0.2 eV	96Bon (special)
O_2 at 400 K (4×10^{-2} mbar) PdO		surface oxide	+1.1 eV	96Bon (special)
PdO			+1.5 eV	97Pil (no fit)

4.3.2.13 Pd(111)

[00Sur] makes use of the coordination number concept (see section 4.3.1). For the example of the c(4×2) structure, the existence of two adsorbate-induced features in the Pd $3d_{5/2}$ core level favors a structural model with fcc and hcp hollow sites over a bridge site model. While the bridge-only model would only yield one adsorbate related feature, the hollow sites model has Pd atoms bonded to one CO molecule only (H_1) and Pd atoms bonded to two CO molecules (H_2). Therefore, H_1 corresponds to 1/3 Pd-CO coordination (CO shared by three Pd atoms), H_2 corresponds to 2/3 Pd-CO (two "1/3-CO molecules" bound to Pd) (=associated with occupation of both fcc and hcp sites, different to H_1 not because of site but because of coordination), on-top has coordination number 1 (one CO per Pd). Again, as for the Pd(100) surface, a linear relationship between coordination number and shift is observed, from 0.37 eV (1/3) to 0.7 eV (2/3) to 1.05 eV (1). Bridge (1/2) features as expected at 0.5 eV. We want to mention that the binding energies of the different components display some very small shifts (some meV) upon increasing the CO coverage. Shown are only the values for coverages closest to the nominal values of the observed adsorbate structures.

Pd $3d_{5/2}$ level, E_b(bulk)			334.9 eV	98San, 00Sur (D-S+G) 00Lei (Sci)
Clean surface				
			–0.28 eV	98San, 94And2, 00Sur (D-S+G)
			–0.3 eV	00Lei (Sci)
CO adsorption				
(√3×√3)R30° fcc hollow H_1	1/3	0.33 ML	+0.34 eV	00Sur (D-S+G)
c(4×2)-2CO hollow H_1	1/3	0.50 ML	+0.40 eV	00Sur (D-S+G)
c(4×2)-2CO hollow H_2	2/3	0.50 ML	+0.69 eV	00Sur (D-S+G)
(2×2)-3CO hollow H_2	2/3	0.75 ML	+0.75 eV	00Sur (D-S+G)
(2×2)-3CO on-top	1	0.75 ML	+1.05 eV	00Sur (D-S+G)
(2×2)-CO bridge	1/2	0.75 ML	+0.52 eV	00Sur (D-S+G)
(√3×√3)R30° hollow (300 K)		> 0.1 ML	+0.32 eV	00Sur (D-S+G)
CO bridge (300 K)		> 0.1 ML	+0.59 eV	00Sur (D-S+G)
O adsorption				
(2×2) hollow (300 K)		0.25 ML	+0.32 eV	00Lei (Sci)
CO coadsorption on (2×2)-O				
CO induced core-level shift			+0.40 eV	00Lei (Sci)
C_2H_2 adsorption				
(√3×√3)R30° hollow		0.33 ML	+0.58 eV	98San (D-S+G)
(2×2) hollow		0.21 ML	+0.58 eV	98San (D-S+G)
C_2H_3 adsorption				
(√3×√3)R30°		0.33 ML	+0.72 eV	98San (D-S+G)
H adsorption				
(1×1)			> 0 eV	98San (no fit)

4.3.2.14 Ta(100)

In a theoretical study, Krakauer has calculated a clean SCLS of +0.96 eV for the first and no shift for the second layer [84Kra]. Since no final state effects are taken into account, the agreement seems reasonable. A better agreement is found in [85Gui] by using a microscopic model, where for the 1st layer a value of +0.9 eV and for the 2nd layer +0.14 eV is found for the unrelaxed surface. If some relaxation is included, both values are reduced by about 0.05 eV.

Ta $4f_{7/2}$ level, E_b(bulk)			21.65 eV	84Gui2, 85Gui, 85Spa (D-S+G)
Clean surface				
1st layer 2nd layer			+0.74 eV +0.14 eV	84Gui2, 85Gui, 85Spa (D-S+G)
O adsorption				
O chemisorbed		low coverage	+0.99 eV	84Gui2 (D-S+G)
O oxide-like		higher coverage	+1.29 eV	84Gui2 (D-S+G)
H adsorption				
H		low coverage	+0.93 eV	84Gui2 (D-S+G)
Cs adsorption				
not specified			+0.64 eV	85Sou (D-S+G)

4.3.2.15 Ta(110)

[95Ruc] uses the Ta $4f_{5/2}$ level to derive the shifts, since the components of the 7/2 level overlap with the 5/2 peak.

In [94And1] no adsorbate induced component is observed, but the position of the clean surface component is shifting with increasing coverage. This shift is coverage-dependent and non-linear. For saturation coverages the quoted values are obtained.

Theoretical calculations of the clean SCLS yield 0.4 eV [85Gui].

Ta $4f_{7/2}$ level, E_b(bulk)			21.65 eV 21.58 eV	84Gui2, 85Gui (D-S+G) 94And1 (no fit)
Clean surface				
			+0.28 eV	85Gui (D-S+G)
			+0.3 eV	95Ruc (no fit)
			+0.31 eV	94And1 (no fit)
1st layer 2nd layer			+0.360 eV +0.065 eV	93Rif (D-S+G)
O adsorption				
O chemisorbed p(2×1) [81Tre]			+1.1 eV	95Ruc (no fit)
monolayer oxide [81Tre]		(both coexist)	+1.9 eV	95Ruc (no fit)
bulk oxide Ta_2O_5			+4.5 eV	95Ruc (no fit)
Alkali adsorption				
Na - surface component		saturation	+0.355 eV	94And1 (no fit)
Rb - surface component		saturation	+0.330 eV	94And1 (no fit)

4.3.2.16 Ta(111)

Oxygen adsorption on Ta(111) at room temperature leads to monolayer adsorption for exposures up to 1 L and to various oxidation states for higher exposures [82Vee]. State "A" is related to the adsorbate phase, while "C" and "D" are related to different sub-oxides. For hydrogen adsorption, continuous shifts of the clean surface components are observed [82Vee].

Published calculations of the clean surface core-level shift give very large shifts of +0.86 eV for the first and 0.14 eV for the 2nd layer [85Gui].

Ta $4f_{7/2}$ level, E_b(bulk)			21.64 eV	82Vee (D-S+G)
Clean surface				
1st layer 2nd layer			+0.4 eV +0.19 eV	82Vee (D-S+G)
1st layer 2nd layer			+0.39 eV +0.11 eV	84Wer (D-S+G)
O adsorption				
O A			+1.12 eV	82Vee (D-S+G)
O C			+1.3 eV	82Vee (D-S+G)
O D			+2.4 eV	82Vee (D-S+G)
H adsorption				
1st layer surface component 2nd layer surface component		saturation saturation	+0.65 eV +0.36 eV	82Vee (D-S+G)

4.3.2.17 Ta (poly)

[84Him] reported an oxidation study of polycrystalline Ta. In order to identify oxidation states, different oxidation procedures have been used; average values are presented here. Fairly mild conditions lead to adsorbate phases or surface oxides.

Ta $4f_{7/2}$ level, E_b(bulk)				
Clean surface				
O adsorption				
oxidation state +1			+0.48 eV	84Him (no fit)
oxidation state +3			+1.22 eV	84Him (no fit)
oxidation state +5			+2.05 eV	84Him (no fit)
oxidation state +5 in bulk oxide			+5.2 eV	84Him (no fit)

4.3.2.18 W(100)

The clean surface, which has a (1×1) structure at room temperature, is reconstructed in a c(2×2) structure at low temperatures [81Vee2, 89Jup, 96Jup, 93Mul]. While [81Vee2] attributed two surface related components to unreconstructed (S1) and reconstructed (S2) domains, later publications identified these peaks with 1st and 2nd layer W atoms, the former of which exhibit a small shift upon reconstruction [84Gui1, 89Jup, 93Mul, 96Jup].

For hydrogen adsorption the new position of the original surface components of clean W(100) is noted. No additional H induced features are observed [81Vee2, 82Vee]. In [81Vee2] the S1 component vanishes for H coverages above 0.1 ML, while the S2 component gradually shifts to lower binding energies; however, at saturation H coverages, where the reconstruction is completely lifted, S2 does not reach the binding energy of the clean surface S1 component. In contrast, in the work of Guillot et al. [82Gui], two pairs of peaks are used without allowing for a shift.

Theoretical calculations of the SCLS are included in [99Kim] for the clean and the Li or K covered surfaces. In [85Gui] values of –0.55 and –0.23 eV are reported for the clean SCLS of the 1st and 2nd layer atoms, respectively.

W $4f_{7/2}$ level, E_b(bulk)			31.42 eV 31.41 eV 31.5 eV 31.44 eV	82Vee (V) 81Vee2 (V) 86Jup, 96Jup (D-S+G) 85Spa (D-S+G) 93Mul (D-S+G)
Clean surface				
			–0.35 eV	82Vee (V)
			–0.36 eV	84Wer (D-S+G)
			–0.4 eV	85Spa (D-S+G)
unreconstructed (S1) reconstructed (S2)			–0.35 eV –0.13 eV	81Vee2 (V)
1st layer high temp. (1×1) low temp. (2×2) 2nd layer			–0.37 eV –0.35 eV –0.14 eV	89Jup,96Jup (D-S+G)
1st layer high temp (1×1) low temp. (2×2) 2nd layer			–0.40 eV –0.35 eV –0.16 eV	84Gui1 (D-S+G)
1st layer (2×2) (1×1) 2nd layer			–0.35 eV –0.45 eV –0.11 eV	93Mul (D-S+G)
1st layer 2nd layer			–0.39 eV –0.19 eV	86Jup (D-S)
1st layer unreconstructed 2nd layer			–0.4 eV –0.16 eV	82Gui (special)
O adsorption				
O chemisorbed p(2×1)		0.5 ML	+0.53 eV	82Vee (V)
O chemisorbed		0.6 ML	+0.53 eV	89Aln (special)
2D reconstr. oxide		1.0 ML	+1.3 … +1.4 eV	89Aln (special)
WO_2			+1.7 ... +1.8 eV	89Aln (special)
O induced (110) facets (900 K)		>1.25 ML	+0.7 eV	89Aln (special)
H adsorption				
surface component		saturation	–0.255 eV	82Vee (V)
c(2×2) (S2)		<0.2 ML	–0.14 eV	81Vee2 (V)
p(1×1) (S2)		>0.8 ML	–0.25 eV	81Vee2 (V)
c(2×2) 1st layer 2nd layer		0.5 ML	–0.25 eV –0.09 eV	82Gui (special)
p(1×1) 1st layer 2nd layer		saturation	–0.32 eV –0.15 eV	82Gui (special)
W bound to H (unrecon. dom.) 2nd layer W pinched surf. molecules W_2H			–0.22 eV –0.10 eV +0.06 eV	96Jup (D-S+G)
Cs adsorption				
		0.1 ML	–0.35 eV	85Sou (D-S+G)
p(2×2)		0.57 ML	–0.46 eV	85Sou (D-S+G)

S adsorption				
p(2×2) (1S/W)		0.25 ML	–0.25 eV	93Mul (D-S+G)
c(2×2) (2S/W)		0.5 ML	+0.07 eV	93Mul (D-S+G)
N adsorption				
c(2×2) fourfold hollow – S1		<0.3 ML	–0.09 eV	86Jup (D-S)
c(2×2) fourfold hollow – S2			+0.18 eV	86Jup (D-S)
c(2×2) fourfold hollow – S3			+0.41 eV	86Jup (D-S)
Li adsorption				
1st layer		0<θ<0.5 ML >0.5 ML	–0.32…–0.50 eV –0.50 eV	99Kim (D-S+G)
2nd layer		0<θ<1.0 ML	–0.15…–0.20 eV	99Kim (D-S+G)
K adsorption				
1st layer		0<θ<1.0 ML	–0.32 eV	99Kim (D-S+G)
2nd layer		0<θ<1.0 ML	–0.15…–0.11 eV	99Kim (D-S+G)

4.3.2.19 W(110)

The system O/W(110) has been studied in some detail. The result is a fairly complicated spectral decomposition [98Rif]. The various components given in the table below can be attributed to W surface atoms bonded to varying numbers of O atoms, which are all located in threefold hollow sites. "O1" describes W atoms bonded to one oxygen atom, "O2" describes W atoms bonded to two O atoms, and "O3" are W atoms with three oxygen neighbors. Even more details can be observed. "O1a" denotes the W atom labelled "A" in Fig. 5, while "O1b" represents atom "B". The p(2×1) structure with a coverage of 0.5 ML ideally consists of "O1b" and "O2" surface atoms only, while at a coverage of 0.75 ML (with a p(2×2) structure) "O2" and "O3" atoms are observed. For 1 ML a p(1×1) structure with "O3" surface atoms only has been found [98Rif]. Since usually domains of certain surface structures develop consecutively, mixed phases are observed. In [98Rif] binding energy positions of the various components have been allowed to vary within certain boundaries, giving rise to slightly coverage-dependent core-level shifts, even for the clean surface component. The range of values is reflected in the table by values for certain coverages.

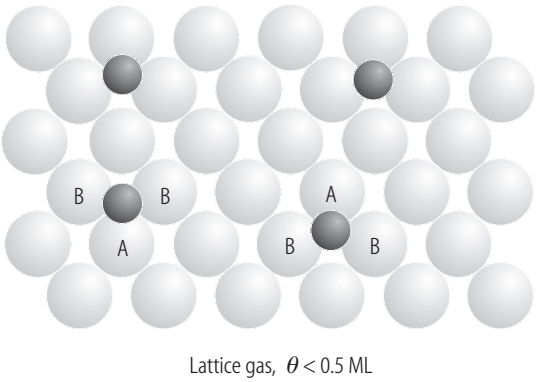

Fig. 5. Surface model describing special W surface atoms. Reproduced from [98Rif].

In [00Ynz] the two different O1 components have not been resolved separately from the bulk. They are included in a single component named "bulk+O1".

For hydrogen adsorption, a H-induced surface reconstruction of the W substrate is found to be one reason for the H-induced core-level shifts. In addition, there is a chemical effect on the binding energies as well [90Rif]. The result is a continuous shift of the H-induced component with increasing coverage. [83Gui] gives an alternative analysis with fixed binding energy positions. They then use three H induced features, namely for W atoms bound to one, two and three H atoms. For completeness we include their attempt with a shifting component summarizing the 1 H and 2 H components as well.

In [94And1] for alkali adsorption, no adsorbate induced component is observed, but the position of the clean surface component is shifting with increasing coverage. This shift is coverage-dependent and non-linear. For saturation coverages the quoted values are obtained.

In a theoretical study a value of –0.30 eV was found for the clean surface core-level shift [01Cho], in good agreement with the experimental data. A similar value (–0.28 eV) has already been reported by [85Gui]. In addition, Oguchi calculated a core-level shift of +0.60 eV for the (1×1)-O adsorbate layer [99Ogu].

W $4f_{7/2}$ level, E_b(bulk)			31.4 eV 31.42 eV 31.5 eV	98Rif, 90Rif, 98Tun (D-S+G) 94Ped (V) 94And1 (no fit) 85Spa (D-S+G) 83Gui (special)
Clean surface				
		average low cov. 0.34 ML	–0.3 eV –0.32 eV –0.29 eV	98Rif (D-S+G)
			–0.32 eV	00Ynz, 94And1
			–0.321 eV	90Rif (D-S+G)
			–0.3 eV	94Ped (V) 83Gui (special)
			–0.30 eV	85Spa (D-S+G) 79Tra (no fit)
			–0.320 eV	98Tun (D-S+G)
			–0.29 eV	89Pur (D-S+G)
O adsorption				
O1a			–0.16 eV	98Rif (D-S+G)
O1b		low cov. 0.34 ML 0.5 ML	–0.08 eV +0.08 eV +0.059 eV	98Rif (D-S+G)
O2		low cov. 0.5 ML	+0.28 eV +0.34 eV	98Rif (D-S+G)
O2		0.2 ML	+0.26 eV	00Ynz (Sci)
O3		0.5 ML	+0.66 eV	98Rif (D-S+G)
p(2×1) O2		0.5 ML	+0.345 eV	00Ynz (Sci)
p(2×2) O2		0.75 ML	+0.365 eV	00Ynz (Sci)
p(2×1) O3		0.5 ML	+0.63 eV	00Ynz (Sci)
p(2×2) O3		0.75 ML	+0.73 eV	00Ynz (Sci)
(1×1)×12 O3		1 ML	+0.73 eV	00Ynz (Sci)
p(2×1) 3-fold sites		0.5 ML	+0.3 eV	94Ped (V)
(1×1)-like		1 ML	+0.6 … +0.7 eV	94Ped] (V)
(1×1)		1 ML	+0.73 eV	98Dai1, 98Dai2
isolated O		small	–0.1 eV	81Tre (G)
p(2×1)		0.5 ML	+0.32 eV	81Tre (G)
oxide (?)		high	+0.6 eV	81Tre (G)

H adsorption				
p(2×1)		0 to 0.5 ML	–0.32 … –0.26 eV	90Rif (D-S+G)
p(1×1) (reconstr.)		0.5 to 1ML	–0.26 … –0.07 eV	90Rif (D-S+G)
isolated H (bound to 2 H)		cov. dep.	–0.22 … –0.08 eV	83Gui (special)
W bound to 1 H W bound to 2 H			–0.22 eV –0.08 eV	83Gui (special)
p(2×1) (bound to 3 H)			+0.2 eV	83Gui (special)
Alkali adsorption				
Na – surface component		saturation	–0.350 eV	94And1 (no fit)
Cs – surface component		saturation	–0.340 eV	94And1 (no fit)
K – surface component		saturation	–0.330 eV	94And1 (no fit)
Ba		> 0.7 ML	–0.400 eV	98Tun (D-S+G)

4.3.2.20 W(111)

For the clean surface two different fitting approaches were used in [87Pur]: a two-peak model with only one "underlayer" peak with a larger width as the surface peak, and a three-peak model with two "underlayer" peaks (2nd and 3rd layer) with the same width. Since the quality of the fit increases and since a different shift for the 2nd layer seems plausible, the authors prefer the three-peak model. For comparison, we display values for both models.

There is a striking difference between H and O adsorption. While for H adsorption the original surface components for 1st and 2nd layer shift by the displayed amounts, a new feature appears for oxygen adsorption. In addition, the original surface component for the 1st layer shifts as well, but its intensity vanishes [82Vee].

The theoretically predicted values for the clean SCLS are –0.43 eV for the 1st layer, –0.20 eV for the 2nd layer and –0.10 eV for the 3rd layer [85Gui].

W $4f_{7/2}$ level, E_b(bulk)			31.42 eV	81Vee1, 82Vee (D-S+G)
Clean surface				
1st layer 2nd layer			–0.43 eV –0.10 eV –0.11 eV	81Vee1, 82Vee, 84Wer, 87Pur (D-S+G) 81Vee1, 82Vee (D-S+G) 84Wer,87Pur (D-S+G)
1st layer 2nd layer 3rd layer			–0.46 eV –0.36 eV –0.11 eV	87Pur (D-S+G)
O adsorption				
O chemisorbed (disordered)			+0.41 eV	81Vee1, 82Vee (D-S+G)
H adsorption				
1st layer surface component		saturation	–0.26 eV	81Vee1, 82Vee
2nd layer surface component		saturation	0	81Vee1, 82Vee

4.3.2.21 W(320) and other stepped W

In [89Pur] three stepped W surfaces have been investigated. The nomenclature for the sites distinguishes between terrace rows, rows on top of the steps (upper row), rows at the bottom of the steps (lower row) and 2nd layer contributions.

The evaluation in [84Cha] assumed, that the terrace atoms show the same SCLS as on the flat W(110) surface. With this constraint the other positions were fitted. The rows in this publication are counted from the upper row of the steps, yielding three (110) rows, a row before the edge row and the edge row itself (lower step row).

A theoretical calculation considering the differently coordinated W atoms on the (320) surface yields results which are giving the same trends in core-level shift, but still with small offset relative to experiment [01Cho].

W $4f_{7/2}$ level, E_b(bulk)			31.5 eV 31.39 eV	84Cha (D-S+G) 89Pur (D-S+G)
Clean surface				
		average	–0.140 eV	94Rif (n.s.)
S1 (3 rows/terr) S2 (2 rows/terr) (3 line fit)			–0.270 eV –0.080 eV	94Rif (n.s.)
S1 S2 S3 (4 line fit)			–0.310 eV –0.200 eV –0.190 eV	94Rif (n.s.)
steps (row 1, upper row) terrace (row 2,3,4) (110) row 5 (last row before edge edge (row 6, lower row)			–0.580 eV –0.300 eV –0.440 eV –0.180 eV	84Cha (D-S+G)
(320) - steps (upper row) - steps (lower row) - terrace (110) - 2nd layer			–0.41 eV –0.25 eV –0.25 eV –0.10 eV	89Pur (D-S+G)
(610) - steps (upper row) - steps (lower row) - terrace (100) - 2nd layer			–0.38 eV –0.28 eV –0.38 eV –0.12 eV	89Pur (D-S+G)
(310) - steps (upper row) - steps (lower row) - 2nd layer			–0.43 eV –0.29 eV –0.12 eV	89Pur (D-S+G)

4.3.2.22 W (poly)

[84Him] reported an oxidation study of polycrystalline W. In order to identify oxidation states, different oxidation procedures and even bulk oxide samples (WO_2 and WO_3) have been used. In the table average values for the different samples are presented. Fairly mild conditions lead to adsorbate phases or surface oxides.

W $4f_{7/2}$ level, E_b(bulk)				
Clean surface				
O adsorption				
oxidation state +2			+0.71 eV	84Him (no fit)
oxidation state +4			+1.62 eV	84Him (no fit)
oxidation state +6			+2.7 eV	84Him (no fit)
oxidation state +6 in bulk oxide			+4.3 eV	84Him (no fit)

4.3.2.23 Os(0001)

Os $4f_{7/2}$ level, E_b(bulk)			50.74 eV	89Mar (D-S+G)
Clean surface				
			–0.41 eV	89Mar (D-S+G)
CO adsorption				
(√3×√3)R30°		0.33 ML	–0.33 eV	89Mar (D-S+G)

4.3.2.24 Ir(100)

The Ir(100) surface can be prepared in a reconstructed and a (1×1) metastable phase. Interestingly, different SCLS are observed for these surfaces. By comparing with the Ir(111) surface (included here), a close relation between the reconstructed Ir(100)-(5×1) and the (111) surface is found [80Vee]. In order to account for instrumental broadening, a triangular function was convoluted with the D-S function.

Ir $4f_{7/2}$ level, E_b(bulk)			60.7 eV	80Vee (D-S)
Clean surface				
(5×1)			–0.49 eV	80Vee (D-S)
(1×1) metastable			–0.68 eV	80Vee (D-S)
(111) surface			–0.50 eV	80Vee (D-S)
H adsorption				
H on (1×1)			0	80Vee (D-S)

4.3.2.25 Ir(110)

Ir $4f_{7/2}$ level, E_b(bulk)			60.7 eV	89Duc (D-S+G)
Clean surface				
(1×2)			–0.5 eV	89Duc (D-S+G)
CO adsorption				
(√3×√3)R30°		0.33 ML	–0.35 eV	89Duc (D-S+G)

4.3.2.26 Ir(332)

The Ir(332) surface consists of six rows of terrace atoms of (111) orientation and single atomic steps with $(11\bar{1})$ orientation. Therefore, the terrace SCLS is very similar to the value for the flat Ir(111) surface (see also Sect. 4.3.2.24). Upon dosing of molecular hydrogen, only the step sites are covered with hydrogen, causing their binding energy to shift to the value for the clean terrace atoms [81Vee3].

Ir $4f_{7/2}$ level, E_b(bulk)				
Clean surface				
terrace step (111)			–0.48 eV –0.75 eV –0.53 eV	81Vee3 (D-S+G)
H adsorption				
step adsorption (H_2 exposure)			–0.48 eV	81Vee3 (D-S+G)

4.3.2.27 Pt(110)

The two publications mainly listed here, foremost differ in the excitation source used. While [89Duc] used a laboratory source, [87Duc] depends on synchrotron data. However, since the laboratory source is a specially made Y Mζ anode with a photon energy of 132.3 eV, a very good surface sensitivity is achieved [86Duc]. The clean Pt(110) surface exhibits a (1×2) reconstruction, which is of the missing-row type. In the (1×1) phase one can distinguish Pt atoms on the rows from Pt atoms in the valleys between. In the case of (1×2), these valleys are twice as deep as for (1×1) and there are row atoms, facet atoms, and valley atoms [87Duc]. For CO adsorption in the p2mg structure the reconstruction is lifted and CO bonds on top of row atoms. The second component observed is related to the valley Pt atoms, which are obviously also affected by the CO adsorption. If CO is adsorbed at low temperatures (≤110 K), the (1×2) reconstruction of the substrate is preserved [87Duc].

Pt $4f_{7/2}$ level, E_b(bulk)			71.1 eV 70.83 eV	87Duc (D-S+G) 82Bae (special) 89Duc (D-S+G)
Clean surface				
(1×2)			–0.46 eV	87Duc (D-S+G)
(1×2)			–0.44 eV	89Duc (D-S+G)
(1×2) - row atoms - valley atoms			–0.55 eV –0.21 eV	82Bae (special)
CO adsorption				
p1g1 (p2mg) on (1×1) - row atoms		1 ML	+0.84 eV	87Duc (D-S+G)
p1g1 (p2mg) on (1×1) - valley atoms			+0.5 eV	87Duc (D-S+G)
on (1×2) - row atoms			+0.8 eV	87Duc (D-S+G)
on (1×2) - facet atoms			+0.35 eV	87Duc (D-S+G)
unspecified			+0.66 eV	89Duc (D-S+G)
H adsorption				
on (1×2) - row/facet atoms on (1×2) - facet/valley atoms			–0.28 eV +0.35 eV	87Duc (D-S+G)
O_2 adsorption				
on (1×2) - row/facet atoms on (1×2) - valley atoms			–0.31 eV +0.31 eV	87Duc (D-S+G)
O adsorption				
on (1×2)		0.9 ML	+0.55 eV	87Duc (D-S+G)
Alkali adsorption				
K		>0.25 ML 0.16 ML 0.05…0.1 ML	–0.12 eV –0.32 eV –0.41 eV	89Duc (D-S+G)
coadsorption				
K (0.25 ML) + CO (saturation)			+0.74 eV	89Duc (D-S+G)

4.3.2.28 Pt(111)

NO/Pt(111) is a case, where the coordination number approach does not explain the observed core-level shifts [03Zhu]. The reason might be the different bonding configuration as compared to CO. H_1 marks Pt atoms bonded to one NO molecule in fcc hollow position, while H_2 is related to Pt atoms bonded to two NO molecules in hcp and fcc hollow sites.

[82Bae] reported an interesting behavior upon oxygen adsorption at high temperatures (900 °C). Although oxygen was detected on the surface, no change in the Pt 4f core level was found. The authors explain this by formation of subsurface oxygen.

Pt $4f_{7/2}$ level, E_b(bulk)			70.90 eV 71.1 eV 70.87 eV 71.09 eV 71.0 eV	94Bjo, 95Pug (Sci) 02Rad (D-S+G) 82Bae, 83Apa (special) 86Duc (D-S+G) 88Leg (D-S+G) 02Kin, 03Zhu (D-S+G)
Clean surface				
			–0.40 eV	94Bjo, 95Pug (D-S+G) 82Apa, 83Apa (special) 82Bae (special)
			–0.37 eV	86Duc, 96Jan, 01Jan
			–0.4 eV	02Rad, 03Zhu (D-S+G)
			–0.42 eV	88Leg (D-S+G)
CO adsorption				
c(4×2) on top	1	0.5 ML	+1.01 eV	94Bjo (Sci)
			+1.0 eV	02Kin (D-S+G)
			+0.9 eV	02Rad (D-S+G)
c(4×2) bridge	1/2	0.5 ML	+0.33 eV	94Bjo (Sci)
			+0.4 eV	02Kin (D-S+G)
			+0.35 eV	02Rad (D-S+G)
15 L		no saturation	+1.0 eV	83Apa (special)
CO unspecified		saturation	+0.63 eV	86Duc (D-S+G)
CO unspecified		saturation	+0.9 eV	82Bae (special)
NO adsorption				
(2×2)-NO fcc hollow H_1		0.25 ML	+0.2 eV	03Zhu (D-S+G)
(2×2)-2NO on-top T		0.50 ML	+0.5 eV	03Zhu (D-S+G)
(2×2)-3NO fcc/hcp hollow H_2		0.75 ML	+0.7 eV	03Zhu (D-S+G)
O adsorption				
(2×2) hollow		0.25 ML	+0.22 eV	94Bjo (Sci)
(2×2) hollow		0.25 ML	+0.2 eV	95Pug (Sci)
O_2 at 700 K (2×2)		surface oxide	+0.75 eV	88Leg (D-S+G)
O_2 adsorption				
phys. phase (25 K)		0.33 ML	–0.4 eV	95Pug (Sci)
chem. phase I hollow (90 K)		0.23 ML	+0.4 eV	95Pug (Sci)
chem. phase II hollow/bridge (138 K)		0.15 ML	+0.3 eV	95Pug (Sci)
C_2H_4 adsorption				
monolayer at 30 K			+0.28 eV	95Her1 (Sci)
monolayer at 90 K			+0.14 eV	95Her1 (Sci)
C_2H_3 adsorption				
C_2H_3 „2×2“ 90 K			+0.4 eV	95Her2 (Sci)
C_2H_3 hollow (2×2)			+0.36 eV	94Bjo (Sci)
C_3H_6 adsorption				
C_3H_6 monolayer 100 K			+0.26 eV	01Jan (D-S+G)
C_4H_6O adsorption				
C_4H_6O monolayer			+0.27 eV	01Jan (D-S+G)

K adsorption				
unspecified			+0.3 eV	83Apa (special)

4.3.2.29 Stepped Pt surfaces

In this subsection measurements reported for different stepped surfaces are summarized. These results clearly demonstrate that the very narrow 4f lines can be well resolved.

Pt $4f_{7/2}$ level, E_b(bulk)			71.1 eV 71.08 eV	83Apa (special) 88Leg (D-S+G)
Clean surface				
Pt(557) terrace			–0.30 eV	83Apa (special)
Pt(557) step			–0.60 eV	83Apa (special)
Pt(557) (unres.)			–0.39 eV	88Leg (D-S+G)
Pt(331) terrace			–0.30 eV	83Apa (special)
Pt(331) step			–0.57 eV	83Apa (special)
CO adsorption				
Pt(331) step		no saturation	+0.7 eV	83Apa (special)
NH_3 adsorption				
Pt(331) step		saturation	+0.15 eV	83Apa (special)
O adsorption				
Pt(557) - O_2 at 700 K (2×2) “surface oxide”			+0.71 eV	88Leg (D-S+G)
Pt(557) - O_2 at 700 K (2×2) “bulk oxide” - PtO_x			+1.2 eV	88Leg (D-S+G)

4.3.2.30 Au(100)

Au $4f_{7/2}$ level, E_b(bulk)			83.99 eV	81Hei (L)
Clean surface				
(5×20) surface (1×1) surface (metastable)			–0.28 eV –0.38 eV	81Hei (L)

4.3.2.31 Au(110)

Au $4f_{7/2}$ level, E_b(bulk)			83.83 eV 83.99 eV	89Duc (D-S+G) 81Hei (L)
Clean surface				
			–0.35 eV	89Duc (D-S+G)
(2×1) surface			–0.35 eV	81Hei (L)
CO adsorption				
saturation		0.3 ML	+0.77 eV	89Duc (D-S+G)
Alkali adsorption				
K			0	89Duc (D-S+G)

4.3.2.32 Au(111)

Au $4f_{7/2}$ level, E_b(bulk)			83.99 eV	81Hei (L)
Clean surface				
			–0.35 eV	81Hei (L)

4.3.2.33 Au (poly)

Au $4f_{7/2}$ level, E_b(bulk)			84.00 eV	78Cit (D-S+G)
Clean surface				
			–0.399 eV	78Cit (D-S+G)

4.3.3 References

70Don Doniach, S., Šunjić, M.: J. Phys. C **3** (1970) 285.

78Bac Bachrach, R.Z., Flodström, S.A., Bauer, R.S., Hagström, S.B.M., Chadi, D.J.: J. Vac. Sci. Technol. **15** (1978) 488.

78Cit Citrin, P.H., Wertheim, G.K., Baer, Y.: Phys. Rev. Lett. **41** (1978) 1425.

78Ebe Eberhardt, W., Kunz, C.: Surf. Sci. **75** (1978) 709.

78Flo Flodström, S.A., Martinsson, C.W.B., Bachrach, R.Z., Hagström, S.B.M., Bauer, R.S.: Phys. Rev. Lett. **40** (1978) 907.

79Bia Bianconi, A., Bachrach, R.Z., Hagström, S.B.M., Flodström, S.A.: Phys. Rev. B **19** (1979) 2837.

79Ebe Eberhardt, W., Himpsel, F.J.: Phys. Rev. Lett. **42** (1979) 1375.

79Sea Seah, M.P., Dench, W.A.: Surf. Interface Anal. **1** (1979) 2.

79Tra Tran Minh Duc, Guillot, C., Lassailly, Y., Lecante, J., Jugnet, Y., Vedrine, J.C.: Phys. Rev. Lett. **43** (1979) 789.

80Joh Johansson, B., Mårtensson, N.: Phys. Rev. B **21** (1980) 4427.

80Ros Rosengren, A., Johansson, B.: Phys. Rev. B **22** (1980) 3706.

80Vee Veen, J.F. van der, Himpsel, F.J., Eastman, D.E.: Phys. Rev. Lett. **44** (1980) 189.

81Hei Heimann, P., Veen, J.F. van der, Eastman, D.E.: Solid State Commun. **38** (1981) 595.

81Kra Krakauer, H., Posternak, M., Freeman, A.J., Koelling, D.D.: Phys. Rev. B **23** (1981) 3859.

81Nyh Nyholm, R., Mårtensson, N., Lebugle, A., Axelsson, U.: J. Phys. F **11** (1981) 1727.

81Tre Treglia, G., Desjonqueres, M.C., Spanjaard, D., Lassailly, Y., Guillot, C., Jugnet, Y., Duc, T.M., Lecante, J.: J. Phys. C **14** (1981) 3463.

81Vee1 Veen, J.F. van der, Heimann, P., Himpsel, F.J., Eastman, D.E.: Solid State Commun. **37** (1981) 555.

81Vee2 Veen, J.F. van der, Himpsel, F.J., Eastman, D.E.: Solid State Commun. **40** (1981) 57.

81Vee3 Veen, J.F. van der, Eastman, D.E., Bradshaw, A.M., Holloway, S.: Solid State Commun. **39** (1981) 1301.

81Wim Wimmer, E., Weinert, M., Freeman, A.J., Krakauer, H.: Phys. Rev. B **24** (1981) 2292.

82Apa Apai, G., Baetzold, R.C., Shustorovich, E., Jaeger, R.: Surf. Sci. **116** (1982) L191.

82Bae Baetzold, R.C., Apai, G., Shustorovich, E., Jaeger, R.: Phys. Rev. B **26** (1982) 4022.

82Fei Feibelman, P.J.: Phys. Rev. B **26** (1982) 5347.

82Gui Guillot, C., Thuault, C., Jugnet, Y., Chauveau, D., Hoogewijs, R., Lecante, J., Tran Minh Duc, Treglia, G., Desjonqueres, M.C., Spanjaard, D.: J. Phys. C **15** (1982) 4023.

82Vee Veen, J.F. van der, Himpsel, F.J., Eastman, D.E.: Phys. Rev. B **25** (1982) 7388.

83Apa Apai, G., Baetzold, R.C., Jupiter, P.J., Viescas, A.J., Lindau, I.: Surf. Sci. **134** (1983) 122.

83Cit Citrin, P.H., Wertheim, G.K.: Phys. Rev. B **27** (1983) 3176.

83Ege Egelhoff jr., W.F.: Phys. Rev. Lett. **50** (1983) 587.

83Gui Guillot, C., Treglia, G., Lecante, J., Spanjaard, D., Desjonqueres, M.C., Chauveau, D., Jugnet, Y., Tran Minh Duc: J. Phys. C **16** (1983) 1555.

83Joh Johansson, B., Mårtensson, N.: Helv. Phys. Acta **56** (1983) 405.

84Cha Chauveau, D., Roubin, P., Guillot, C., Lecante, J., Treglia, G., Desjonqueres, M.C., Spanjaard, D.: Solid State Commun. **52** (1984) 635.

84Ege Egelhoff jr., W.F.: Phys. Rev. B **30** (1984) 1052.

84Gui1 Guillot, C., Desjonqueres, M.C., Chauveau, D., Treglia, G., Lecante, J., Spanjaard, D., Tran Minh Duc: Solid State Commun. **50** (1984) 393.

84Gui2 Guillot, C., Roubin, P., Lecante, J., Desjonqueres, M.C., Treglia, G., Spanjaard, D., Jugnet, Y.: Phys. Rev. B **30** (1984) 5487 (and references therein).

84Him Himpsel, F.J., Morar, J.F., McFeely, F.R., Pollak, R.A., Hollinger, G.: Phys. Rev. B **30** (1984) 7236.

84Kra Krakauer, H.: Phys. Rev. B **30** (1984) 6834.

84Wer Wertheim, G.K., Citrin, P.H., Veen, J.F. van der: Phys. Rev. B **30** (1984) 4343.

85Ege Egelhoff jr., W.F.: J. Vac. Sci. Technol. A **3** (1985) 1305.

85Gui Guillot, C., Chauveau, D., Roubin, P., Lecante, J., Desjonqueres, M.C., Treglia, G., Spanjaard, D.: Surf. Sci. **162** (1985) 46.

85Sou Soukiassian, P., Riwan, R., Coustry, J., Lecante, J., Guillot, C.: Surf. Sci. **152-153** (1985) 290.

85Spa Spanjaard, D., Guillot, C., Desjonqueres, M.-C., Treglia, G., Lecante, J.: Surf. Sci. Rep. **5** (1985) 1.

86Duc Dückers, K., Bonzel, H.P., Wesner, D.A.: Surf. Sci. **166** (1986) 141.

86Ege Egelhoff jr., W.F.: Surf. Sci. Rep. **6** (1986) 253.

86Jup Jupille, J., Purcell, K.G., King, D.A.: Solid State Commun. **58** (1986) 529.

87Duc Dückers, K., Prince, K.C., Bonzel, H.P., Chab, V., Horn, K.: Phys. Rev. B **36** (1987) 6292.

87Pur Purcell, K.G., Jupille, J., Derby, G.P., King, D.A.: Phys. Rev. B **36** (1987) 1288.

88Leg Légaré, P., Lindauer, G., Hilaire, L., Maire, G., Ehrhardt, J.-J., Jupille, J., Cassuto, A., Guillot, C., Lecante, J.: Surf. Sci. **198** (1988) 69.

88Mar Mårtensson, N., Stenborg, A., Björneholm, O., Nilsson, A., Andersen, J.N.: Phys. Rev. Lett. **60** (1988) 1731.

88Nil Nilsson, A., Eriksson, B., Mårtensson, N., Andersen, J.N., Onsgaard, J.: Phys. Rev. B **38** (1988) 10357.

89Aln Alnot, P., Auerbach, D.J., Behm, J., Brundle, C.R., Viescas, A.: Surf. Sci. **213** (1989) 1.

89Duc Dückers, K., Bonzel, H.P.: Surf. Sci. **213** (1989) 25.

89Jup Jupille, J., Purcell, K.G., King, D.A.: Phys. Rev. B **39** (1989) 6871.

89Mar Mårtensson, N., Saalfrank, H.B., Kuhlenbeck, H., Neumann, M.: Phys. Rev. B **39** (1989) 8181.

89Pur Purcell, K.G., Jupille, J., King, D.A.: Surf. Sci. **208** (1989) 245.

89Ste1 Stenborg, A., Björneholm, O., Nilsson, A., Mårtensson, N., Andersen, J.N., Wigren, C.: Surf. Sci. **211/212** (1989) 470.

89Ste2 Stenborg, A., Björneholm, O., Nilsson, A., Mårtensson, N., Andersen, J.N., Wigren, C.: Phys. Rev. B **40** (1989) 5916.

90Rif Riffe, D.M., Wertheim, G.K., Citrin, P.H.: Phys. Rev. Lett. **65** (1990) 219.

91And Andersen, J.N., Qvarford, M., Nyholm, R., Sorensen, S.L., Wigren, C.: Phys. Rev. Lett. **67** (1991) 2822.

91Bag Bagus, P.S., Pacchioni, G., Parmigiani, F.: Phys. Rev. B **43** (1991) 5172.

91Com Comelli, G., Sastry, M., Paolucci, G., Prince, K.C., Olivi, L.: Phys. Rev. B **43** (1991) 14385.

91Nyh Nyholm, R., Andersen, J.N., Acker, J.F. van, Qvarford, M.: Phys. Rev. B **44** (1991) 10987.

92And Andersen, J.N., Lundgren, E., Nyholm, R., Qvarford, M.: Phys. Rev. B **46** (1992) 12784.

92Nyh Nyholm, R., Qvarford, M., Andersen, J.N., Sorensen, S.L., Wigren, C.: J. Phys. Condens. Matter **4** (1992) 277.

93And Andersen, J.N., Lundgren, E., Nyholm, R., Qvarford, M.: Surf. Sci. **289** (1993) 307.

93Bag Bagus, P.S., Pacchioni, G.: Phys. Rev. B **48** (1993) 15262.

93Ber Berg, C., Raaen, S., Borg, A., Andersen, J.N., Lundgren, E., Nyholm, R.: Phys. Rev. B **47** (1993) 13063.

93Lun Lundgren, E., Johansson, U., Nyholm, R., Andersen, J.N.: Phys. Rev. B **48** (1993) 5525.

93Mul Mullins, D.R., Lyman, P.F.: Surf. Sci. **285** (1993) L473.

93Nil Nilsson, A., Stenborg, A., Tillborg, H., Gunnelin, K., Martensson, N.: Phys. Rev. B **47** (1993) 13590.

93Rif Riffe, D.M., Wertheim, G.K.: Phys. Rev. B **47** (1993) 6672.

94Ald Alden, M., Abrikosov, I.A., Johansson, B., Rosengaard, N.M., Skriver, H.L.: Phys. Rev. B **50** (1994) 5131.

94And1 Andrews, A.B., Riffe, D.M., Wertheim, G.K.: Phys. Rev. B **49** (1994) 8396.

94And2 Andersen, J.N., Hennig, D., Lundgren, E., Methfessel, M., Nyholm, R., Scheffler, M.: Phys. Rev. B **50** (1994) 17525.

94Bjo Björneholm, O., Nilsson, A., Tillborg, H., Bennich, P., Sandell, A., Hernnäs, B., Puglia, C., Mårtensson, N.: Surf. Sci. **315** (1994) L983.

94Bor Borg, A., Berg, C., Raaen, S., Venvik, H.J.: J. Phys.: Condens. Matter **6** (1994) L7.

94Gur Gürer, E., Klier, K., Simmons, G.W.: Phys. Rev. B **49** (1994) 14657.

94Loc Locatelli, A., Brena, B., Lizzit, S., Comelli, G., Cautero, G., Paolucci, G., Rosei, R.: Phys. Rev. Lett. **73** (1994) 90.

94Ped Peden, C.H.F., Shinn, N.D.: Surf. Sci. **312** (1994) 151.

94Pri Prince, K.C., Santoni, A., Morgante, A., Comelli, G.: Surf. Sci. **317** (1994) 397.

94Rif Riffe, D.M., Kim, B., Erskine, J.L., Shinn, N.D.: Phys. Rev. B **50** (1994) 14481.

95And Andersen, J.N., Lundgren E., Nyholm R.: J. Electron Spectrosc. Relat. Phenom. **75** (1995) 225.
95Her1 Hernnäs, B.: Ph. D. Thesis, Uppsala University 1995, paper IV: Hernnäs, B., Nilsson, A., Karis, O., Puglia, C., Sandell, A., Mårtensson, N.
95Her2 Hernnäs, B.: Ph. D. Thesis, Uppsala University 1995, paper V: Hernnäs, B., Nilsson, A., Karis, O., Puglia, C., Sandell, A., Mårtensson, N.
95Mar Mårtensson, N., Nilsson, A.: Application of Synchrotron Radiation, Eberhard, W.(ed.), Springer Ser. Surf. Sci. **35** (1995) 65.
95Pug Puglia, C., Nilsson, A., Hernnäs, B., Karis, O., Bennich, P., Mårtensson, N.: Surf. Sci. **342** (1995) 119.
95Ruc Ruckman, M.W., Qiu, S.-L., Strongin, M.: Appl. Surf. Sci. **89** (1995) 401.
96Bon Bondzie, V.A., Kleban, P., Dwyer, D.J.: Surf. Sci. **347** (1996) 319.
96Ham Hammer, B., Morikawa, Y., Norskov, J.K.: Phys. Rev. Lett. **76** (1996) 2141.
96Jan Janin, E., Björkqvist, M., Grehk, T.M., Göthelid, M., Pradier, C.-M., Karlsson, U.O., Rosengren, A.: Appl. Surf. Sci. **99** (1996) 371.
96Jup Jupille, J., Purcell, K.G., King, D.A.: Surf. Sci. **367** (1996) 149.
96Loc Locatelli, A., Brena, B., Comelli, G., Lizzit, S., Paolucci, G., Rosei, R.: Phys. Rev. B **54** (1996) 2839.
96Par Park, K.T., Simmons, G.W., Klier, K.: Surf. Sci. **367** (1996) 307.
96Zac Zacchigna, M., Astaldi, C., Prince, K.C., Sastry, M., Comicioli, C., Rosei, R., Quaresima, C., Ottaviani, C., Crotti, C., Antonini, A., Matteucci, M., Perfetti, P.: Surf. Sci. **347** (1996) 53.
97Beu Beutler, A., Lundgren, E., Nyholm, R., Andersen, J.N., Setlik, B., Heskett, D.: Surf. Sci. **371** (1997) 381.
97Fad Fadley, C.S., Chen, Y., Couch, R.E., Daimon, H., Denecke, R., Denlinger, J.D., Galloway, H., Hussain, Z.,. Kaduwela, A.P, Kim, Y.J., Len, P.M., Liesegang, J., Menchero, J., Morais, J., Palomares, J., Ruebush, S.D., Rotenberg, E., Salmeron, M.B., Scalettar, R., Schattke, W., Singh, R., Thevuthasan, S., Tober, E.D., Van Hove, M.A., Wang, Z., Ynzunza, R.X.: Prog. Surf. Sci. **54** (1997) 341.
97Pil Pillo, Th., Zimmermann, R., Steiner, P., Hüfner, S.: J. Phys. Condens. Matter **9** (1997) 3987.
97Pri Prince, K.C., Ressel, B., Astaldi, C., Peloi, M., Rosei, R., Polcik, M., Crotti, C., Zacchigna, M., Comicioli, C., Ottaviani, C., Quaresima, C., Perfetti, P.: Surf. Sci. **377-379** (1997) 117.
97Ram Ramsey, M.G., Leisenberger, F.P., Netzer, F.P., Roberts, A.J., Raval, R.: Surf, Sci. **385** (1997) 207.
97Sti Stichler, M., Wurth, W., Menzel, D., Denecke, R., Fadley, C.S.: Advanced Light Source Compendium of User Abstracts, 1997 (LBNL-41658).
98Beu Beutler, A., Lundgren, E., Nyholm, R., Andersen, J.N., Setlik, B.J., Heskett, D.: Surf. Sci. **396** (1998) 117.
98Bih Bihlmayer, G., Eibler, R., Podloucky, R.: Surf. Sci. **402-404** (1998) 794.
98Dai1 Daimon, H., Ynzunza, R., Palomares, J., Takabi, H., Fadley, C.S.: Surf. Sci. **408** (1998) 260.
98Dai2 Daimon, H., Ynzunza, R.X., Palomares, F.J., Tober, E.D., Wang, Z.X., Kaduwela, A.P., Van Hove, M.A., Fadley, C.S.: Phys. Rev. B **58** (1998) 9662.
98Rif Riffe, D.M., Wertheim, G.K.: Surf. Sci. **399** (1998) 248.
98San Sandell, A., Beutler, A., Jaworowski, A., Wiklund, M., Heister, K., Nyholm, R., Andersen, J.N.: Surf. Sci. **415** (1998) 411.
98Str Strisland, F., Ramstad, A., Ramsvik, T., Borg, A.: Surf. Sci. Lett. **415** (1998) L1020.
98Tun Tun-Wen Pi, Ie-Hong Hong, Chiu-Ping Cheng: Phys. Rev. B **58** (1998) 4149.
99Bag Bagus, P.S., Illas, F., Pacchioni, G., Parmigiani, F.: J. Electron Spectrosc. Relat. Phenom. **100** (1999) 215.
99Den Denecke, R., Väterlein, P., Bässler, M., Wassdahl, N., Butorin, S., Nilsson, A., Rubensson, J.-E., Nordgren, J., Mårtensson, N., Nyholm, R.: J. Electron Spectrosc. Relat. Phenom. **101-103** (1999) 971.
99Kim Kim, H.W., Ahn, J.R., Chung, J.W., Yu, B.D., Scheffler, M.: Surf. Sci. **430** (1999) L515.
99Ogu Oguchi, T.: Surf. Sci. **438** (1999) 37.
00Bar1 Baraldi, A., Lizzit, S., Comelli, G., Goldoni, A., Hofmann, P., Paolucci, G.: Phys. Rev. B **61** (2000) 4534.
00Bar2 Baraldi, A., Lizzit, S., Paolucci, G.: Surf. Sci. **457** (2000) L354.

00Lei Leisenberger, F.P., Koller, G., Sock, M., Surnev, S., Ramsey, M.G., Netzer, F.P., Klötzer, B., Hayek, K.: Surf. Sci. **445** (2000) 380.
00Sur Surnev, S., Sock, M., Ramsey, M.G., Netzer, F.P., Wiklund, M., Borg, M., Andersen, J.N.: Surf. Sci. **470** (2000) 171.
00Ynz Ynzunza, R.X., Denecke, R., Palomares, F.J., Morais, J., Tober, E.D., Wang, Z., Garcia de Abajo, F.J., Liesegang, J., Hussain, Z., Van Hove, M.A., Fadley, C.S.: Surf. Sci. **459** (2000) 69.
01And1 Andersen, J.N., Almbladh, C.-O.: J. Phys. Condens. Matter **13** (2001) 11267.
01And2 Andersen, J.N., Balasubramanian, T., Almbladh, C.-O., Johansson, L.I., Nyholm, R.: Phys. Rev. Lett. **86** (2001) 4398.
01Bar Baraldi, A., Lizzit, S., Comelli, G., Paolucci, G.: Phys. Rev. B **63** (2001) 115410.
01Cho Cho, J.-H., Oh, D.-H., Kleinman, L.: Phys. Rev. B **64** (2001) 115404.
01Gan Ganuglia-Pirovano, M.V., Scheffler, M., Baraldi, A., Lizzit, S., Comelli, G., Paolucci, G., Rosei, R.: Phys. Rev. B **63** (2001) 205415.
01Jan Janin, E., Ringler, S., Weissenrieder, J., Åkermark, T., Karlsson, U.O., Göthelid, M., Nordlund, D., Ogasawara, H.: Surf. Sci. **482-485** (2001) 83.
01Liz Lizzit, S., Baraldi, A., Groso, A., Reuter, K., Ganduglia-Pirovano, M.V., Stampfl, C., Scheffler, M., Stichler, M., Keller, C., Wurth, W., Menzel, D.: Phys. Rev. B **63** (2001) 205419.
01Ove Over, H., Seitsonen, A.P., Lundgren, E., Wiklund, M., Andersen, J.N.: Chem. Phys. Lett. **342** (2001) 467.
02Jaw1 Jawarowski, A.J., Asmundsson, R., Uvdal, P., Sandell, A.: Surf. Sci. **501** (2002) 74.
02Jaw2 Jawarowski, A.J., Asmundsson, R., Uvdal, P., Gray, S.M., Sandell, A.: Surf. Sci. **501** (2002) 83.
02Kin Kinne, M., Fuhrmann, T., Whelan, C.M., Zhu, J.F., Pantförder, J., Probst, M., Held, G., Denecke, R., Steinrück, H.-P.: J. Chem. Phys. **117** (2002) 10852.
02Rad Radosavkic, D., Barrett, N., Belkhou, R., Marsot, N., Guillot, C.: Surf. Sci. **516** (2002) 56.
02Woo Woodruff, D.P.: J. Electron Spectrosc. Relat. Phenom. **126** (2002) 55.
03Bar1 Baraldi, A., Lizzit, S., Novello, A., Comelli, G., Rosei, R.: Phys. Rev. B **67** (2003) 205404.
03Bar2 Baraldi, A., Comelli, G., Lizzit, S., Kiskinova, M., Paolucci, G.: Surf. Sci. Rep. **49** (2003) 169.
03Bir Birgersson, M., Almbladh, C.-O., Borg, M., Andersen, J.N.: Phys. Rev. B **67** (2003) 045402.
03Gus Gustafson, J., Borg, M., Mikkelsen, A., Gorovikov, S., Lundgren, E., Andersen, J.N.: Phys. Rev. Lett. **91** (2003) 056102.
03Zhu Zhu, J.F., Kinne, M., Fuhrmann, T., Denecke, R., Steinrück, H.-P.: Surf. Sci. **529** (2003) 384.